A

Thesis Report

on

CNC TOOL PATH IN TERMS OF PARAMETRIC SURFACE

Submitted in partial fulfillment of the requirement for the award of the degree of

Master of Engineering

in

CAD/CAM & Robotics

Submitted By

AMIT KUMAR VERMA

Roll No. 801081003

Under the Guidance of

Dr. JASWINDER SINGH SAINI

Assistant Professor

Mechanical Engineering Department

MECHANICAL ENGINEERING DEPARTMENT

THAPAR UNIVERSITY

PATIALA-147004, INDIA

July-2012

DECLARATION

I hereby declare that the thesis entitled **"CNC TOOL PATH IN TERMS OF PARAMETRIC SURFACE"** is an authentic record of my study carried out as requirement for the award of the degree of **Master of Engineering (CAD/CAM & Robotics)** at **Thapar University, Patiala** under the guidance of **Dr. JASWINDER SINGH SAINI,** Assistant Professor, Department of Mechanical Engineering, Thapar University, Patiala during July 2011 to June 2012. The matter embodied in this report has not been submitted in part or full to any other university or institute for the award of any other degree.

20/7/12

(AMIT KUMAR VERMA)

Reg. No. 801081003

This is to certify that above declaration made by the student concerned is correct to the best of my knowledge & belief.

20/7/12

(Dr. JASWINDER SINGH SAINI)

Assistant professor,

Department of Mechanical Engineering,

Thapar University, Patiala-147004.

Countersigned by:

(Dr. AJAY BATISH)

Professor and Head,

Department of Mechanical Engineering,

Thapar University,

Patiala-147004.

(Dr. S.K. MOHAPATRA)

Dean of Academic Affairs,

Thapar University,

Patiala-147004.

ACKNOWLEDGEMENT

I would like to express a deep sense of gratitude and thank profusely to my guide **Dr. JASWINDER SINGH SAINI** for his sincere & invaluable guidance, suggestions and attitude, which inspired me to submit thesis in the present form. His dynamism and diligent enthusiasm have been highly instrumental in keeping my spirits high. His flawless and forthright suggestions blended with an innate intelligent application have crowned my task with success.

I am also thankful to **Dr. AJAY BATISH,** Professor and Head, Department of Mechanical Engineering for his encouragement and inspiration for execution of the thesis work.

A special thanks to my friend **Mr. Ghansham Goyal** for their valorous help and co-operation.

I am also thankful to other faculty members and all the workshop staff of Mechanical Engineering Department of Thapar University, Patiala for their everlasting support.

Dated: 20-07-12

AMIT KUMAR VERMA

Registration No.: 801081003

ABSTRACT

Freeform surfaces, also called sculptured surfaces, have been widely used in various engineering applications. They are defined as surfaces containing one or more non-planar non-quadratic surfaces generally represented by parametric and/or tessellated models. Freeform surfaces, have been widely used in aerospace, automobile, consumer products and the die/mold industry. Freeform surfaces are usually designed to meet or improve an aesthetic and/or functional requirement. Sculptured surfaces are widely used in the design of complex products with aerodynamic features. These freeform surfaces are often produced by 3-axis Computer Numerical Control (CNC) machine tools using ball-end milling cutters. The utilization of CNC machines to manufacture complex surfaces has driven extensive research work, especially in the area of tool path generation. Various methodologies and computer tools have been developed in the past to improve efficiency and quality of freeform surface machining.

From the literature review, it is found that there are number of different algorithms given by various researchers on the accurate tool path planning of free-form surfaces. The present study discusses the efficient and accurate tool path planning algorithm for smooth free-form surfaces in terms of planar cubic B-spline surface given by Lartigue *et al*. [16]. The procedure begins with interpolation of tool path in terms of cubic B-spline curve, and then computation of maximum scallop height and pick feed such that the maximum scallop height along the scallop curve is within the prescribed tolerance.

As a next step of the present work, verification of the algorithm is done by machining a part on a CNC machine tool.

LIST OF FIGURES

LIST OF TABLES

INDEX

CHAPTER 1
INTRODUCTION

1.1 GENERAL

Machining is a form of subtractive manufacturing, in which a collection of material-working processes utilizing power-driven machine tools, such as saws, lathes, milling machines, and drill presses, are used with a sharp cutting tool to physically remove material to achieve a desired geometry. Machining is the most important of the manufacturing processes. Machining can be also defined as the process of removing material from a workpiece in the form of chips. The term metal cutting is used when the material is metallic.

The three principal machining processes are classified as turning, milling and drilling. Other operations falling into miscellaneous categories include shaping, planning, boring, broaching and sawing. Turning operations are operations that rotate the work piece as the primary method of moving metal against the cutting tool. Lathes are the principal machine tool used in turning. Milling operations are operations in which the cutting tool rotates to bring cutting edges to bear against the work piece. Milling machines are the principal machine tool used in milling. Drilling operations are operations in which holes are produced or refined by bringing a rotating cutter with cutting edges at the lower extremity into contact with the work piece. Drilling operations are done primarily in drill presses but sometimes on lathes or mills. Miscellaneous operations are operations that may not produce chips during machining but these operations are performed at a typical machine tool. Burnishing is an example of a miscellaneous operation. Burnishing produces no chips but can be performed at a lathe, mill, or drill press. More recent, advanced machining techniques like Electrical Discharge Machining (EDM), Electro-Chemical Erosion, Laser Cutting, or Water Jet Cutting are used to shape metal work pieces.

The machining of materials using machines is not very accurate, to some extent, it also depends upon the skill of the worker operating the machine. The production rate on a machine also depends on the work piece. Hence there are compromises in production rate as well as in accuracy. These drawbacks led people moving towards NC/CNC machines. The accuracy is greater as compared to a conventional machine, accuracy of NC/CNC machine depends upon the part program prepared by the programmer. The production rate is also high as compared to the conventional machines. The advantages of the NC/CNC machines increased their usage as compared to the conventional machines.

1.2 NC/CNC MACHINES

Numerical Control (NC) refers to the automation of machine tools that are operated by abstractly programmed commands encoded on a storage medium, as opposed to manually controlled via hand wheels or levers, or mechanically automated via cams alone. The first NC machines were built in the 1940s and 1950s, based on existing tools that were modified with motors that moved the controls to follow points fed into the system on punched tape. These early servomechanisms were rapidly augmented with analog and digital computers, creating the modern Computer Numerical Control (CNC) machine tools that have revolutionized the machining processes.

In modern CNC systems, end-to-end component design is highly automated using Computer Aided Design (CAD) and Computer Aided Manufacturing (CAM) programs. The programs produce a computer file that is interpreted to extract the commands needed to operate a particular machine via a postprocessor, and then loaded into the CNC machines for production. Since any particular component might require the use of a number of different tools-drills, saws, etc., modern machines often combine multiple tools into a single "cell". In other cases, a number of different machines are used with an external controller and human or robotic operators that move the component from machine to machine. In either case, the complex series of steps needed to produce any part is highly automated and produces a part that closely matches the original CAD design. In CNC, a "crash" occurs when the machine moves in such a way that is harmful to the machine, tools, or parts being machined, sometimes resulting in bending or breakage of cutting tools, accessory clamps, vises, and fixtures, or causing damage to the machine itself by bending guide rails, breaking drive screws, or causing structural components to crack or deform under strain. A mild crash may not damage the machine or tools, but may damage the part being machined so that it must be scrapped.

In CNC machine the program is put into the machine and the machine is then ready for production. Some machined components will generally require a number of different tooling applications such as drilling, reaming and tapping etc., and most modern machines will combine tools within a single cell. This cell will move or rotate to apply the required tooling application, and this will also be controlled by the CNC system.

The main benefit of CNC machine is that the cutting process is controlled by a central computer. This eliminates a lot of the human error which can exist with standard machine. The precise nature of computer control means that a lot of the tasks impossible with human controlled are possible with CNC machines. The vertical cutting also can move

along a z-axis, allowing precise methods of cutting (such as engraving), not possible with manual machines. Although originally expensive, CNC machine has dropped in price, thanks to the low cost of computers and open source software.

CNC machines are traditionally programmed using manual part programming consisting of G-codes and M-codes. It is the most common method of programming, some machine-tool/control manufacturers also have invented their own proprietary "conversational" methods of programming, trying to make it easier to program simple parts and make set-up and modifications at the machine easier .These have met with varying success. It is also known as G-code programming. Used mainly in automation, it is part of Computer-Aided Engineering. G-code is sometimes also called G programming language. In decades past G-code was the more common term, and remains such among many users. G-codes are also called preparatory codes, and are any word in a CNC program that activates or prepare the compiles, begins with the letter "G". This includes:

i. Rapid move (transport the tool through space to the place where it is needed for cutting; do this as quickly as possible).
ii. Controlled feed move in a straight line or arc.
iii. Series of controlled feed moves that would result in a hole being bored, a workpiece cut (routed) to a specific dimension, or a profile (contour) shape added to the edge of a workpiece.
iv. Set tool information such as offset.
v. Switch coordinate systems.

M codes are miscellaneous codes used to perform various functions like spindle start/stop, coolant on/off, automatic tool change, end of program etc.

G and M codes are used for the machining of regular surfaces, but for the machining of irregular surfaces or free form surfaces different approaches are developed for the tool path generation. As there are irregularities in the surface the effort is done to plan the tool path efficiently so that no area of the surface remains unmachined.

1.3 FREE FORM SURFACES

The surfaces which are not regular in their shape and are made by joining different patches together by defining some continuity at points of joining are called free form surfaces. Freeform surfaces, also called sculptured surfaces, have been widely used in aerospace, automobile, consumer products and the die/mold industry. Freeform surfaces are usually designed to meet or improve an aesthetic and/or functional requirement. Often they are defined as surfaces containing one or more non-planar, non-quadratic surfaces generally

represented by parametric and/or tessellated models. Freeform surface, or freeform surfacing, is used in CAD and other computer graphics software to describe the skin of a 3D geometric element. Freeform surfaces do not have rigid radial dimensions, unlike regular surfaces such as planes, cylinders and conic etc. They are used to describe forms such as turbine blades, car bodies, boat hulls etc. Initially developed for the automotive and aerospace industries, freeform surfacing is now widely used in all engineering design disciplines from consumer goods products to ships. The smoothness between patches, known as continuity, is often referred to in terms of a C value:

C0: Position Continuity

C1: Tangent continuity

C2: Curvature Continuity

Free form surfaces usually comprise different surfaces joined together by defining any of the above continuity at the joining edges. The different surfaces can be Bezier surface, B-Spline surface, Hermite surface etc.

The next chapter gives a brief literature review of the machining of such free form surfaces.

CHAPTER 2
LITERATURE REVIEW

2.1 INTRODUCTION

Free-form surfaces are widely used in CAD systems to describe the surfaces of parts, such as molds and dies. There are different methods available to machine free form surfaces on CNC machines. Many researchers have worked on different algorithms to machine free form surfaces on CNC machines. The following section gives a brief view of research work performed by different researchers to develop efficient algorithms for generating free form surfaces.

2.2 LITERATURE REVIEW

Wang and Wang [1] presented a method for modeling swept volume by computing a family of critical curves from a moving solid. Based on this approach, a system was developed for real-time verification of NC tool paths using computer graphics.

Loney and Ozsoy [2] created a prototype software package called CISPA (Computer Interactive Surfaces Pre-APT). The system used a menu-driven front end with graphical feedback to guide a user through curve and free form surface definition resulting in a mathematical model which was used to generate NC machine CLSF.

Kuragano *et al.* [3] developed an integrated free-form-shape design and manufacturing system. The system runs on an engineering workstation with a 3D color display. It provided various means for designers to input their ideas and to modify them to develop an aesthetically pleasing free-form shape. The shape was examined using a variety of display techniques, and the system automatically generated collision-free tool paths for rough and fine cuts from the designed shape.

Zhou *et al.* [5] presented an algorithm for computation of the stationary points of the squared distance functions between two point sets. The problem was reformulated in terms of solution of n polynomial equations with n variables expressed in the tensor product Bernstein basis. The solution method was based on subdivision relying on the convex hull property of the n-dimensional Bernstein basis and minimization techniques.

Shpitalni *et al.* [6] presented two realtime interpolation algorithms and compared them with different CAD interpolators. With the new interpolators, the amount of geometric informations transferred from the CAD system to the CNC system was reduced by orders of magnitude. Moreover the contour errors caused by the new interpolators were much

smaller than those caused by conventional CAD interpolators. Here the various possibilities for implementing curve interpolators on CNC machines were analyzed and new schemes were offered.

Yang and Kong [7] presented a comparative study of linear and parametric interpolators used for command generation during CNC machining. A parametric interpolator that was designed for command generation for parametric curves (or surfaces) was used. Two algorithms for the online implementation of this parametric interpolator were introduced. The comparison is mainly based on memory size, feedrate fluctuation and CPU time. Other considerations included tracking errors and jerk magnitude. Results showed that the parametric interpolator was favorable in the machining of free-form geometry in terms of high speed and tight tolerancing.

Maekawa and Patrikalakis [8] described a new robust method to decompose a free form surface into regions with specific range of curvature and provided important tools for surface analysis, tool path generation, and tool size selection for numerically controlled machining, tessellation of trimmed patches for surface interrogation and finite element meshing and fairing of free form surfaces. The key element in these techniques is the computation of all real roots within a finite box of system of nonlinear equations involving polynomials and square roots of polynomials. An accurate and robust method to decompose a Bezier surface patch into sub patches with specific ranges of curvature was proposed. The method was applied to automatic machine-tool size selection and tool-path generation for NC machining, surface interrogation for fairing, and finite element meshing and surface panelization for performance analysis. But the method is applicable to the case when the numbers of stationary points of curvature are finite.

Kim and Kim [9] developed a new CNC tool path planning method for accurate and efficient finishing cutting of sculptured surfaces. The proposed method generated CNC tool paths based on an offset surface of an object instead of the actual surface. The new algorithm consists of two main computational techniques: offset surface generation technique and offset CNC tool path planning technique. In offset surface generation, approximate parametric offset surfaces are generated accurately from an original parametric surface by employing bi-cubic surface patch, surface conversion, and surface subdivision algorithms. In offset CNC tool path planning, the precise geometric models of chordal deviation and cusp height on an offset surface are established. The effectiveness of the proposed CNC tool path planning method was verified by geometric simulation.

Maekawa [10] provided an efficient and reliable method for computing the shortest path

between two points on a free-form parametric surface and the shortest path between a point and a curve on a free-form parametric surface. The problems were reduced to solving a two point boundary value problem. The approach for solving the two point boundary value problem was based on a relaxation method relying on finite difference discretization. Step controlled correction procedure in the Newton's method makes it possible to start with initial vectors which are not necessarily close to the solution vector, which helps to find all the geodesic paths between two points and a point to a curve. But the algorithms failed once the intermediate path goes outside of the parameter domain. This can be fixed by gluing the surface patches to all the four boundaries.

Lin and Koren [11] presented an analytical method for planning an efficient tool-path in machining free-form surfaces on 3-axis milling machines. The method used a non-constant offset of the previous tool-path, which guarantees the cutter moving in an unmachined area of the part surface and without redundant machining. The method comprised three steps: (i) the calculation of the tool-path interval, (ii) the conversion from the path interval to the parametric interval, and (iii) the synthesis of efficient tool-path planning.

Sarma and Dutta [12] proposed a new method for generating NC tool paths. The method gave the part programmer direct control over the scallop height of the manufactured surface. The geometry and spacing of the tool paths impact the scallop height and time of manufacturing respectively. The method also provided options to the part programmer for generating a variety of tool paths based on practical metrics such as tool path length, tool path curvature and number of tool retractions.

Dragomatz and Mann [13] presented the literature related to numerical control milling path generation, drawn from engineering, computer science, and mathematics. The focus was on the work that includes some aspect of path generation, in particular, computing and creating roughing and finishing paths for 2- to 5-axis machine tools.

Hu *et al.* [14] presented a paper to develop robust algorithm for computing interval polynomial curve-to-surface and surface-to-surface intersections. the method reduced the intersection problems into solving balanced or unbalanced systems of non-linear interval polynomial equations.

Ye and Maekawa [15] presented the algorithm for computing the differential geometry properties of intersection curves of two surfaces where the combination of two surfaces can be parametric–parametric, implicit–implicit and parametric–implicit.

Lartigue *et al*. [16] presented an accurate and efficient method to generate a CNC tool path for a smooth free-form surface in terms of planar cubic B-spline curves which were fed into a free-form curve interpolator. Finally the break points are interpolated, which were generated by computing the offset surface-driving plane intersection curve reflecting the curvature, by a planar cubic B-spline curve. The maximum scallop height along a scallop curve by computing the stationary points of the distance function between the scallop curve and the design surface. Furthermore, the maximum pick feed was computed such that the maximum scallop height along a scallop curve coincided with the prescribed tolerance. Since the method does not depend on discrete sampling, approximation in determining the pick feed, nor linear approximation of the offset surface-plane intersection curve, it is more accurate than the conventional method. The use of B-spline representation reduced the memory requirements significantly.

Feng and Huiwen [17] presented an approach for the determination of efficient tool paths in the machining of sculptured surfaces using 3-axis ball end milling. The objective was to keep the scallop height constant across the machined surface such that redundant tool paths were minimized. The present work determined the tool paths without restoring to the approximated 2D representation of the 3D cutting geometry. Two offset surfaces of the design surface, the scallop surface and the tool center surface were employed to successively establish scallop curves on the scallop surface and cutter location tool paths for the design surface. The effectiveness of the approach was demonstrated through the machining of a typical sculptured surface. The results indicated that constant scallop height machining achieved the specified machining accuracy with fewer and shorter tool paths.

Chen and Dejun [19] proposed to generate accurate iso-cusped tool paths for sculptured surface machining on three-axis CNC machines using all types of end mills. The major contributions of the work included simplifying the geometric representation of the cusp with virtual cutting edges and locating the cusp points accurately. In this work, computing the intersection of two planar virtual cutter edges was easier and faster than computing the intersection between two cutter-swept surfaces in the existing methods. Therefore, the approach to generating iso-cusped tool paths for sculptured surface machining can be implemented in CAD/CAM software systems to benefit the manufacturing industry.

Lasemi *et al*. [20] provided a state-of-the-art review on research development in CNC machining of freeform surfaces. The review primarily focused on three aspects in freeform surface machining: tool path generation, tool orientation identification, and tool geometry

selection. For each aspect, first concepts, requirements and fundamental research methods were briefly introduced. In tool path generation, iso-scallop tool paths along with the curvature matching method have significantly lead to the improved surface quality and reduced machining time. Development of optimal tool orientation techniques for 5 axis machining has significantly improved machining productivity and quality. Methods for the tool orientation identification focus on either improvement of the computational efficiency of the existing methods or development of new methods. Tool orientation smoothing plays an important role to achieve a high quality of freeform surface machining.

2.3 PROPOSED WORK

From the literature review mentioned above, it is found that there are number of different algorithms given by various researchers on the accurate tool path planning of free-form surfaces. One such method is given by Lartigue *et al*.[16]. The author presented the algorithms using B-spline curve. So the objective of the present work is to :

(i) Implement the algorithm for free-form curve in C/C++/MATLAB.

(ii) To experimentally validate the algorithm, which was not done in Lartigue *et al.*[16].

CHAPTER 3

In the past computers were slower and support lower computational requirements due to which only linear or circular paths were supported by CNC interpolators. Presently, where computing speed has been increased drastically the research on free-form curve interpolators has become quite active. The free-form parametric curve interpolator accepts all the curve coordinates directly and generates motion commands on-line. Obviously, in comparison with linear interpolator the method given by Lartigue *et al*. [16] is much more accurate and requires less memory. The objective of the work is to create an efficient and accurate tool path planning algorithm for smooth free-form surface. The planar cubic B-spline curve interpolation method is used in which data points are interpolated by planar cubic B-spline curve equation. With reference to Lartigue *et al*. [16] a three-axis CNC machine tool with a ball end-mill cutter is used, where the cutting tool moves simultaneously in the x, y and z direction. We further consider that the rough machining has already been done and the part is subjected to finishing. As discussed in Lartigue *et al*. [16] the algorithm is given as under.

3.1 INTERPOLATION OF TOOL PATH BY CUBIC B-SPLINE

Before starting with formulation, some notations are introduced. Bold letters such as **c** and **S** are used for vectors and vector functions. The dot (scalar) product and cross (vector) product of two vectors, **a** and **b**, are expressed as **a.b** and **a** × **b**, respectively.

The triple scalar product of three vectors **a**, **b** and **c**, (**a** × **b**).**c**, is denoted by det(a, b, c). The prime (′) denotes the differentiation with respect to the arc length *s*, while the dot (**.**) denotes the differentiation with respect to the parameter ***t***, for example $\mathbf{c}'(s) = d\mathbf{c}/ds$, $\mathbf{c}''(s) = d^2\mathbf{c}/ds^2$, $\dot{\boldsymbol{c}}(t) = d\mathbf{c}/dt$. In general, the lower letters such as u, v, used for subscript denote partial derivative with respect to the corresponding variable, for example $\mathbf{r}_u = \partial\mathbf{r}/\partial u$.

First of all, the design surface is taken, which is a regular parametric surface and expressed as $Q(u, v)$, i.e. $|Q_u \times Q_v| \neq 0$ for all (u, v). The offset surface to the design surface $Q(u, v)$ is

$$\widehat{Q}(u, v) = Q(u, v) + dN(u, v) \tag{3.1}$$

where, d is the offset distance and $N(u, v)$ is the unit normal.

$$N(u, v) = \frac{Q_u \times Q_v}{|Q_u \times Q_v|} \tag{3.2}$$

The tool path is generated as a series of intersection curves which are interpolated by B-spline curve. These intersection curves are plotted between the offset surface, and the tool driving

planes. The distance between the offset surface and the design surface is equal to the radius of ball end-mill, R. These tool driving planes and the axis of the machine tool are parallel to each other, as shown in Fig.3.1.

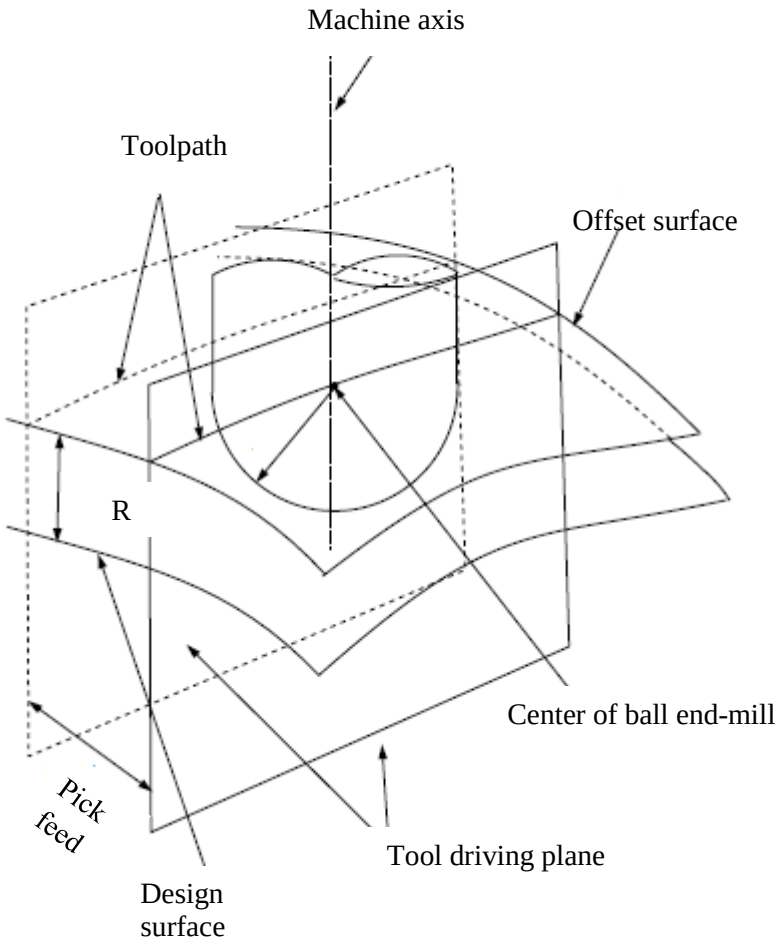

Fig. 3.1. Illustration of offset surface-plane intersection method[16]

Let the x, y, z components of the unit normal vector of the tool driving plane are denoted by α, β,γ , then the equation of the tool driving plane in an implicit form becomes

$$\alpha x + \beta y + \gamma z + \delta = 0 \tag{3.3}$$

When we substitute the x, y, z components of the offset surface given by equation (3.1) with d = R into the driving plane, equation (3.3), The intersection curve is obtained in u-v.

$$f(u, v) = \alpha \hat{x}(u, v) + \beta \hat{y}(u, v) + \gamma \hat{z}(u, v) + \delta = 0 \tag{3.4}$$

The intersection curve can also be viewed as a curve on the two intersecting surfaces. A curve $u = u(t), v = v(t)$ in the uv-plane defines the intersection curve on the offset surface as $r = c(t) = \widehat{\mathrm{Q}}(u(t), v(t))$. It follows that we can rewrite equation (3.4) as$f\big(u(t), v(t)\big) = 0$.

Differentiating this equation with respect to the parameter t ,we get:

$$f_u\dot{u} + f_v\dot{v} = 0 \tag{3.5}$$

The solution to equation (3.5) can also be given by

$$\dot{u} = \xi f_v \ , \ \dot{v} = -\xi f_u \tag{3.6}$$

where ξ is an arbitrary non-zero factor that can be chosen to provide the arc length parametrization. The arc length parameterization is given by:

$$\hat{\mathrm{E}}\dot{u^2} + 2\hat{\mathrm{F}}\dot{u}\dot{v} + \hat{\mathrm{G}}\dot{v^2} = 1 \tag{3.7}$$

where $\hat{\mathrm{E}}, \hat{\mathrm{F}}, \hat{\mathrm{G}}$ are the first fundamental form coefficients of the offset surface and hence

$$\xi = \pm \frac{1}{\sqrt{\hat{\mathrm{E}}f_v^2 - 2\hat{\mathrm{F}}f_u f_v + \hat{\mathrm{G}}f_u^2}} \tag{3.8}$$

For computing the tool path, the points of the intersection curve are computed. These points are computed successively by integrating the nonlinear differential equation (3.6). The starting point is evaluated by solving a univariate nonlinear equation (3.4), where either u or v is fixed. Since there is only one starting point for each single path and we know the approximate location of the starting point, Newton's method[4] can be used to solve the univariate nonlinear equation.

By solving above equations, a sequence of parameter pairs $(u_k, v_k), k = 0,1$ .... are generated which are the ordered set of points along the single tool path when they are substituted into $\hat{\mathrm{Q}}(u, v)$. These sequences of points are interpolated by a planar cubic B-spline curve.

$$\boldsymbol{c}(t_k) = \hat{\mathrm{Q}}(u_k, v_k), k = 0,1 \ldots \ldots \tag{3.9}$$

These sequence of points are also called as ***break points***. If we reduce the number of break points the curve segments which represent the tool path are also reduced. We have to generate the break points according to the curvature of the intersection curve. In the region where the curvature of the intersection curve is large we should generate more break points and in the region where the curvature is small we need to generate less break points. So we need to compute the curvature of the curve first. We compute the curvature of the intersection curve at $\boldsymbol{c}(t_k)$ by using the method [15]. Then the intersection curve is locally approximated by a circular arc with a radius of the computed radius of curvature. We evaluate the step size to obtain the next break point (t_{k+1}) , such that the deviation of the chord $\boldsymbol{c}(t_k)\ \boldsymbol{c}(t_{k+1})$ to the circular arc is thirty times the prescribed tolerance for interpolation ϵ_{tol}. If the step size is larger than four times the tool radius, it is set to four times the tool radius. The numbers thirty and four are based on heuristics. Once the step size is determined, the next break point $\boldsymbol{c}(t_{k+1})$ is obtained by integrating equation (3.6). By repeating this procedure we reach the

other end of the intersection curve. Finally all the evaluated break points are interpolated by a planar cubic B-spline curve. An interpolated curve with break points is illustrated in Fig. 3.2.

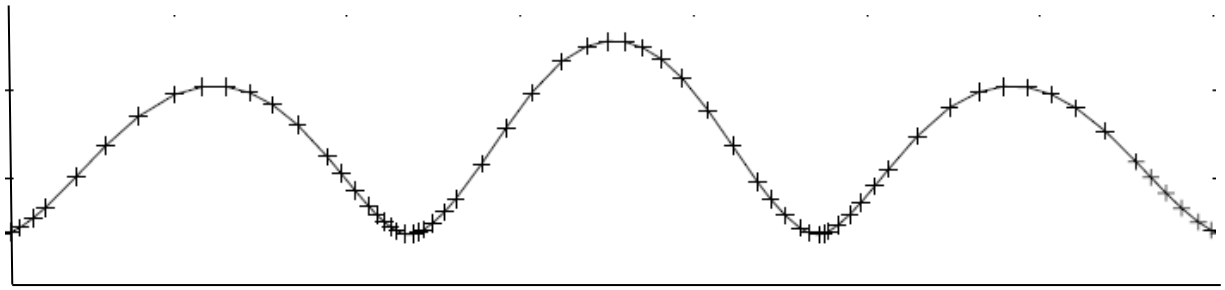

Fig. 3.2. Tool path represented by cubic B-spline[16]

3.2 COMPUTATION OF MAXIMUM SCALLOP HEIGHT

We compute a sequence of approximate intersection points between the offset surface and tool driving planes. These intersection points are interpolated by a planar cubic B-spline curve to the desired accuracy. If the ball end-mill moves along the tool path, the profile of the ball end-mill forms a pipe surface. The two adjacent pipe surfaces intersect along the scallop curve as shown in Fig. 3.3.

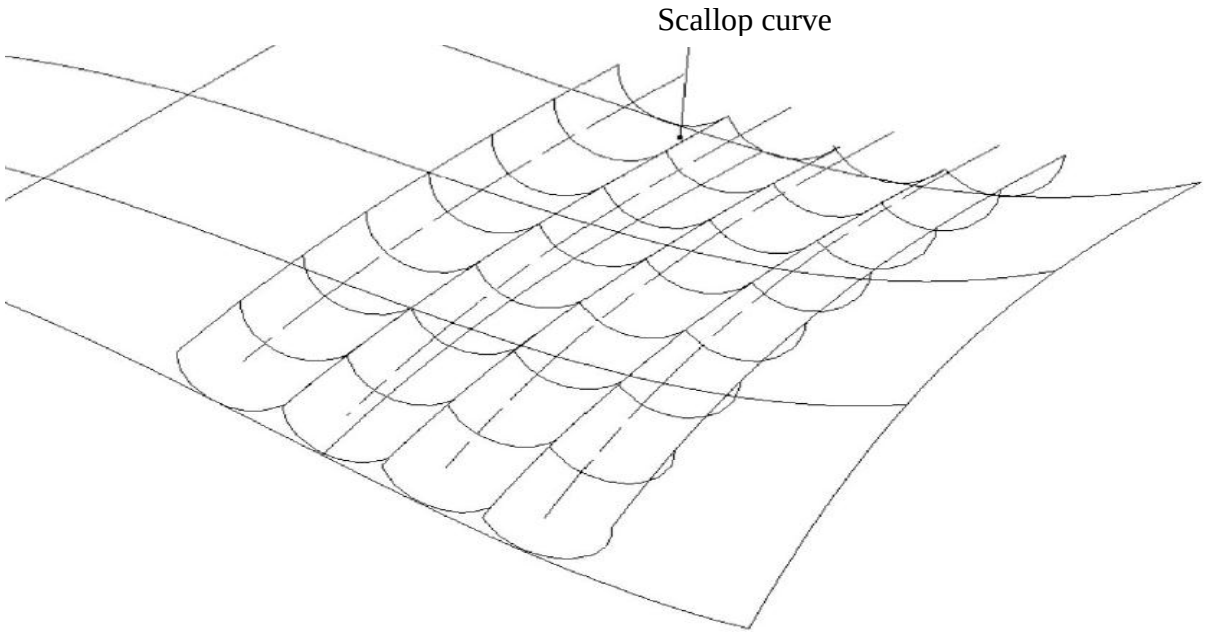

Fig. 3.3. Tool path and scallop curve[16]

The distance between the scallop curve and the design surface is the scallop height, which is the cusp height of the material removed by the cutter, as shown in Fig. 3.4.

The scallop curve is an intersection curve between the two pipe surfaces which are given by

$$P^A(t,\theta) = \boldsymbol{c}^A(t) + R[cos\theta\ n^A(t) + sin\theta\ b^A(t)] \quad (3.10)$$

$$P^B(\sigma,\emptyset) = \boldsymbol{c}^B(\sigma) + R[cos\emptyset\ n^B(\sigma) + sin\emptyset\ b^B(\sigma)] \quad (3.11)$$

where, the spline curves $\boldsymbol{c}^A(t)$ and $\boldsymbol{c}^B(\sigma)$ are the two successive tool paths represented by the cubic B-spline curves. The intersection of the two pipe surfaces(Fig. 3.4) can be described as a three-dimensional vector equation in four unknowns as follows:

$$P^A(t,\theta) = P^B(\sigma,\emptyset) \quad (3.12)$$

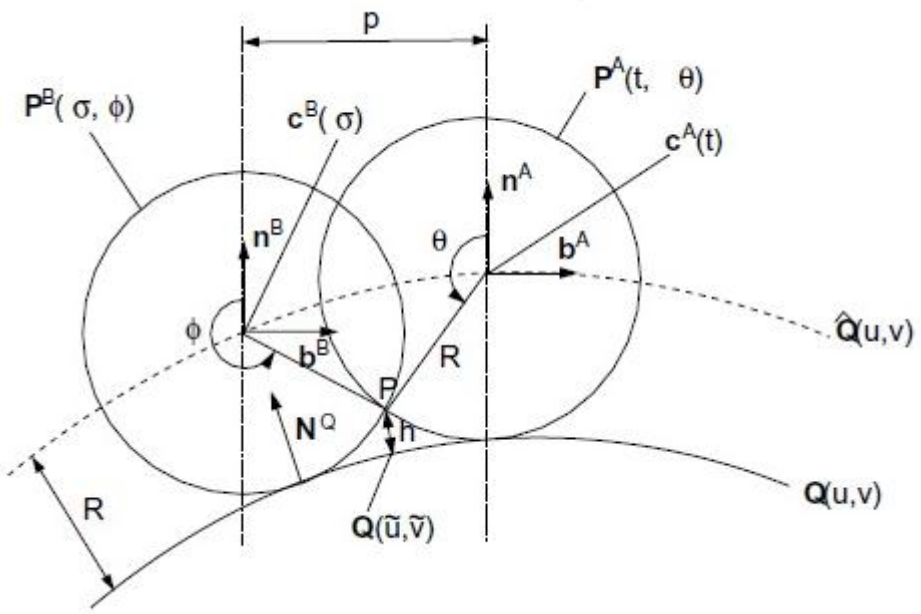

Fig. 3.4 Two pipe surfaces intersecting with scallop height *h* [16]

We can trace the intersection curve of the two parametric pipe surfaces (scallop curve) using a similar technique that we used for tracing the tool path in Section 3.1. When we denote the arc length parametrized scallop curve by $s(s)$, then the tangential direction of $s(s)$ is perpendicular to the normal vectors of both the pipe surfaces at the intersection. We assume that the scallop height is small as compared to the tool radius and hence the two pipe surfaces intersect transversally and therefore the two normal vectors are not parallel to each other. Since $s(s)$ is arc length parametrized, the derivative $s'(s)$ must be a unit vector, hence we have

$$s'(s) = \frac{N^A \times N^B}{\left| N^A \times N^B \right|} \quad (3.13)$$

where, $N^A = P_t^A + P_\theta^A$ and $N^B = P_\sigma^B + P_\emptyset^B$ (3.14)

Differential equations for tracing transversal intersection curves of two parametric surfaces can be derived by differentiating the scallop curve with respect to the parameter s, yielding

$$s' = P_t^A t' + P_\theta^A \theta' \tag{3.15}$$

$$s' = P_\sigma^B \sigma' + P_\emptyset^B \emptyset' \tag{3.16}$$

Since s' is constrained in tangent planes spanned by P_t^A, P_θ^A and $P_\sigma^B, P_\emptyset^B$, eqs (3.15) and (3.16) do not possess normal components and hence equations (3.15) and (3.16) consist of two sets of linear systems in unknowns t′, θ' and σ', $\emptyset'$respectively. By taking the dot product on both sides of equation (3.15) with P_t^A, P_θ^A and eq. (3.16) with P_σ^B, $P_\emptyset^B$ we obtain two sets of linear systems, which can be solved as [14]

$$t' = \frac{\det(\mathrm{N^A}, s', \mathrm{P_\theta^A})}{\mathrm{N^A} \cdot \mathrm{N^A}}, \qquad \theta' = \frac{\det(\mathrm{N}^A, s', P_t^A)}{\mathrm{N}^A \cdot N^A},$$

$$\sigma' = \frac{\det(\mathrm{N}^B, s', P_\emptyset^B)}{N^B \cdot N^B}, \qquad \emptyset' = \frac{\det(N^B, s', P_\sigma^B)}{N^B \cdot N^B} \tag{3.17}$$

where s' is given by equation (3.13). This system of four first-order ordinary differential equations can be solved numerically as an initial value problem. We choose the step size as $\Delta s = (R/M)$, where R is the tool radius and M is an integer. The initial and terminal values of t , θ, σ and $\emptyset$ can be obtained by fixing either t or σ in equation (3.12) (t_{fix} and σ_{fix} are 0 or 1) and solving the system by Newton's method[4]. The initial values for Newton's iteration are given by computing the orthogonal projection of, $c^A(t_{fix})$ onto $c^B(\sigma)$ to find the parameter value s and by the trigonometry.

$$\theta = \pi - \tan^{-1} \frac{p}{2(R - h_{tol})} \tag{3.18}$$

where, h_{tol} is the allowable tolerance and p is the pick feed between the previous and the current tool paths and $\emptyset = 2\pi - \theta$ (see Fig.3.4). The integration generates a sequence of parameter pairs (t_k, θ_k) and $(\sigma_k, \emptyset_k)$ at position s_k along the scallop curve which yield an ordered set of points

$$s(s_k) = P^A(t_k, \theta_k) = P^B(\sigma_k, \emptyset_k) \text{ for } k = 0, 1, 2 \ldots \tag{3.19}$$

The scallop height is considered as the minimum distance between the scallop curve $s(s)$, where the parameter s is an arc length, and the design surface $\mathrm{Q}(u, v)$. The squared distance function between the s(s) and the $\mathrm{Q}(u, v)$ in three dimensional Cartesian space is defined by

$$D(s, u, v) = | s(s) - \mathrm{Q}(u, v) |^2 = (s(s) - \mathrm{Q}(u, v)) \cdot (s(s) - \mathrm{Q}(u, v)) \tag{3.20}$$

The stationary points of $D(s, u, v)$ satisfy the following equations [5]

$$D_s(s, u, v) = 0, D_u(s, u, v) = 0, D_v(s, u, v) = 0 \tag{3.21}$$

which can be rewritten using equation (3.20) as

$$f(s,u,v) = \big(s(s) - \mathrm{Q}(u,v)\big) \cdot s'(s) = 0 \quad (3.22)$$

$$g(s,u,v) = \big(s(s) - \mathrm{Q}(u,v)\big) \cdot \mathrm{Q}_u(u,v) = 0 \quad (3.23)$$

$$h(s,u,v) = \big(s(s) - \mathrm{Q}(u,v)\big) \cdot \mathrm{Q}_v(u,v) = 0 \quad (3.24)$$

The equations (3.22)-(3.24) in s,u,v can be solved by using Newton's method[4]. It is assumed that there is only one stationary point within the length of the tool radius along the tool path. Therefore, we set the initial values as

$s_{k+1} = s_k + M\Delta s \ \big(k = 0,1 \ldots \ and \ \Delta s = (R/M)\big)$,

where the corresponding (u_k, v_k) is obtained by computing the orthogonal projection of s(s_k)(equation (3.19)) onto $\mathrm{Q}(u,v)$. For applying Newton's method[4] we need to evaluate $(t,\theta,\sigma,\emptyset)$ at position s which does not coincide with the integrated points s_k. Therefore, we integrate the equation (3.17) from the closest integrated point s_k to the position s. A stationary point can be classified into a local maximum, local minimum, or saddle point. A typical scallop curve deviation from the design surface formed by two successive paths (Fig. 3.5(a)) is plotted in Fig. 3.5(b) by sampling some points along the scallop curve.

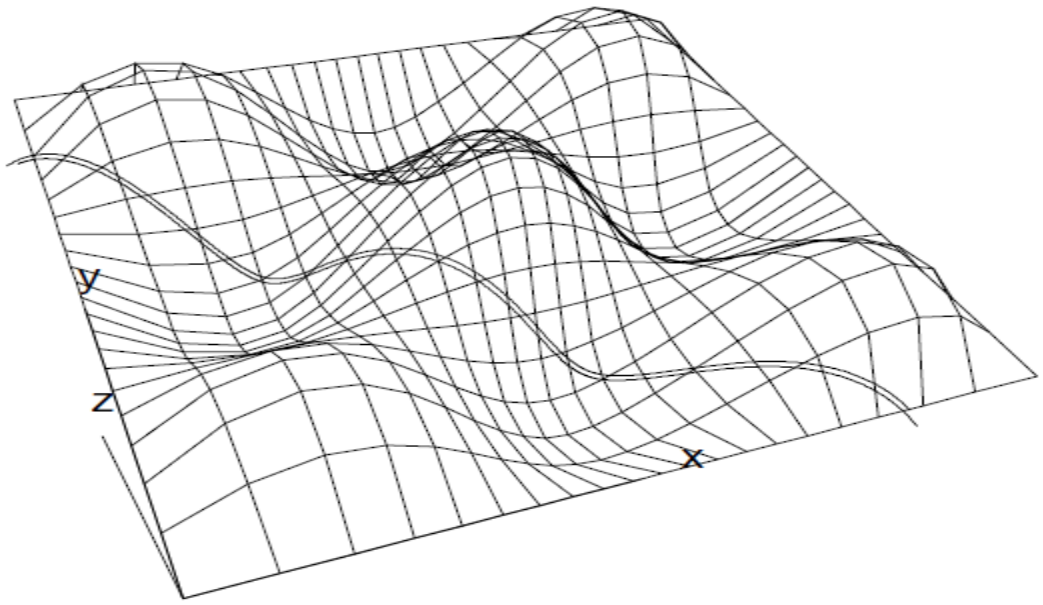

Fig. 3.5(a) Two successive tool paths on a wave-like surface[16]

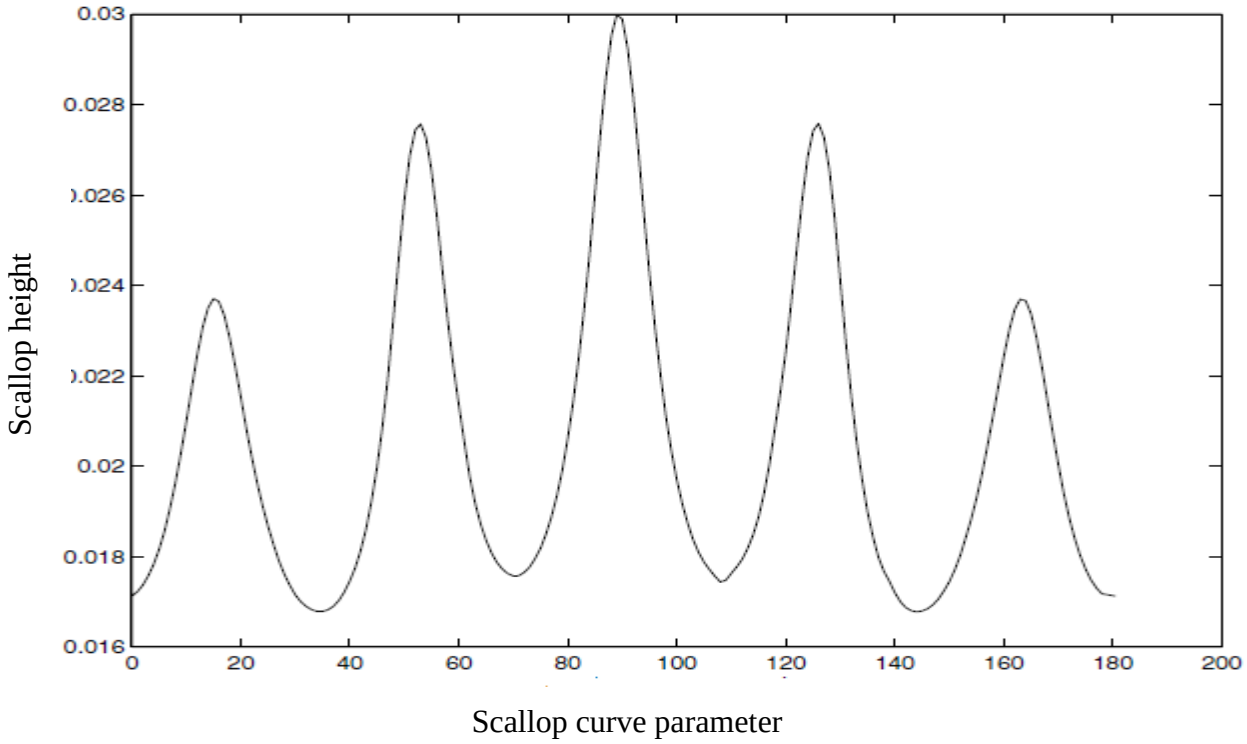

Fig.3.5(b) The deviation of the scallop curve from the design surface generated by the two successive tool paths[16]

We can easily observe that there exist five local maxima and six minima along the scallop curve. To find a global maximum, we select the maximum value among all the local maxima and the values at two end points.

3.3 DETERMINATION OF MAXIMUM PICK FEED

Pick feed is the interval between two successive parallel planes, as shown in Fig.3.1.

For the efficient tool path we have to determine the maximum pick feed such that the maximum scallop height coincides with the prescribed tolerance, h_{tol}. Let the current and the next tool paths are represented by c^A, c^B respectively. Further, we denote the parameter value on the current tool path corresponding to the maximum scallop height of the scallop curve, which is denoted by t_{max} and its corresponding point on the scallop curve which is denoted by P.

We first determine the angle θ such that the scallop height at P (Fig. 3.4) becomes the prescribed tolerance h_{tol} :

$$h(\theta) = | P^A(t_{max}, \theta) - \tilde{Q}(u, v) | = h_{tol} \quad (3.25)$$

where, $\tilde{Q}(u, v)$ is a footpoint of the orthogonal projection of $P^A(t_{\max}, \theta)$ onto the design surface $\tilde{Q}(u, v)$. Equation (3.25) can be solved by Newton's method[4] where the initial

approximation for θ is given by equation (3.18). Here the unknown pick feed is approximately computed by the previous pick feed. We then compute the next tool path by interpolating the sequence of points :

$c^B(\sigma_k) = Q(u_k, v_k)\ k = 0, 1. \ . \ .$

Here we also replaced the unknown pick feed by the previous pick feed to evaluate the tool driving plane. The parameter value σ of $c^B(\sigma)$which forms the maximum scallop height at P with $c^A(t_{max})$ can be computed by finding an orthogonal projection of $c^A(t_{max})$ onto $c^B(\sigma)$ and is denoted by σ_{max} If we denote the solution of equation (3.25) as θ_{max}, we deduce the following three-dimensional vector equation

$$F(f, u, v) = P^A(t_{max}, \theta_{max}) - (Q(u, v) + RN^Q(u, v) + R(\cos\emptyset n^B + \sin\emptyset b^B)) \quad (3.26)$$

in three unknowns $\emptyset$, u, v, where the vector Q (u, v) + R$N^Q(u, v)$ indicates the center of the pipe surface $P^B(\sigma, \emptyset)$ and $n^B and\ b^B$ are the normal and binormal vectors of the tool path at $\sigma = \sigma_{max}$ (Fig.3.4). The initial approximations of u, v, $\emptyset$ for Newton's iteration may be obtained by linearly interpolating (σ_k, u_k, v_k) for $\sigma = \sigma_{max}$ and setting $\emptyset = 2\pi - \theta$ For each iteration, we update the pick feed p by

$$p = \alpha H \cdot i + \beta H \cdot j + \gamma H \cdot k \quad (3.27)$$

where i, j, k are the unit vectors along the coordinate axes and H = $c^A(t_{max}) - c^B(\sigma_{max})$. Then we construct the new tool path $P^B(\sigma, \emptyset)$ based on the new pick feed and iterate until scallop height is within the prescribed tolerance. Once Newton's iteration converges, we compute the maximum scallop height of the new scallop curve and its corresponding parameter value $\bar{t}_{max}$using the technique described in Section 3.2. If $\bar{t}_{max}$ does not match with t_{max} within the prescribed tolerance, we repeat the process from equation (3.25) by replacing t_{max} with $\bar{t}_{max}$.

3.4 GENERATION OF FREE FORM SURFACE

First of all we follow the procedure to develop a free form surface. In this method B-Spline surface equation is used. The design surface is given by equation (3.28)

$$Q(u, v) = \sum_{i=0}^{n} \sum_{j=0}^{m} P_{ij}\ N_{i,k}(u)\ N_{j,l}(v) \qquad 0 \le u \le u_{max} \text{ and } 0 \le v \le v_{max} \quad (3.28)$$

Where

$n + 1$ = control points in u direction

$m + 1$ = control points in v direction

$k-1=$ degree in u direction

$l-1=$ degree in v direction

If we assume a cubic degree surface with four control points in u and v direction then

$n+1=4$

$n=3$

$m+1=4$

$m=3$

$k-1=3$

$k=4$

$l-1=3$

$l=4$

Expanding the equation (3.28)

$$\begin{aligned}Q(u,v) =& P_{00}N_{0,4}(u)N_{0,4}(v)+ P_{01}N_{0,4}(u)N_{1,4}(v)+ P_{02}N_{0,4}(u)N_{2,4}(v)+ P_{03}N_{0,4}(u)N_{3,4}(v)+\\ & P_{10}N_{1,4}(u)N_{0,4}(v)+ P_{01}\ N_{1,4}(u)N_{1,4}(v)+ P_{02}\ N_{1,4}(u)N_{2,4}(v)+ P_{03}\ N_{1,4}(u)N_{3,4}(v)+\\ & P_{20}N_{2,4}(u)N_{0,4}(v)+ P_{01}\ N_{2,4}(u)N_{1,4}(v)+ P_{02}\ N_{2,4}(u)N_{2,4}(v)+ P_{03}\ N_{2,4}(u)N_{3,4}(v)+\\ & P_{30}N_{3,4}(u)N_{0,4}(v)+ P_{01}\ N_{3,4}(u)N_{1,4}(v)+ P_{02}\ N_{3,4}(u)N_{2,4}(v)+ P_{03}\ N_{3,4}(u)N_{3,4}(v)\end{aligned} \quad (3.29)$$

where, $N_{i,k}(u)$ and $N_{j,l}(v)$ are the B-spline functions given by

$$N_{i,k}(u) = (u-t_i)\frac{N_{i,k-1}}{t_{i+k-1}} + (t_{i+k}-u)\frac{N_{i+1,k-1}}{t_{i+k}-t_{i+1}} \quad (3.30)$$

$$N_{j,l}(v) = (v-t_j)\frac{N_{j,l-1}}{t_{j+l-1}} + (t_{j+l}-v)\frac{N_{j+1,l-1}}{t_{j+l}-t_{j+1}} \quad (3.31)$$

for k=1

$$N_{i,1} = f(x) = \begin{cases}1, & t_i \le u \le t_{i+1}\\ 0, & \text{otherwise}\end{cases}$$

where t_i are the knot values given by

$$t_i = f(x) = \begin{cases}0 & i<k\\ i-k+1 & k \le i \le n\\ n-k+2 & i>n\end{cases} \quad ; \quad 0 \le i \le n+k \quad (3.32)$$

Using equation (3.22), the knot values for the assumed conditions are given in table 3.1.

$t_0 = 0$	$t_4 = 1$
$t_1 = 0$	$t_5 = 1$
$t_2 = 0$	$t_6 = 1$
$t_3 = 0$	$t_7 = 1$

Table 3.1. Knot values

The B-spline functions are now calculated as:

Calculation for k=1

$$N_{0,1} = \begin{cases} 1 & t_0 \le u \le t_1 \\ 0 & \text{otherwise} \end{cases} = 1$$

$$N_{1,1} = \begin{cases} 1 & t_1 \le u \le t_2 \\ 0 & \text{otherwise} \end{cases} = 1$$

$$N_{2,1} = \begin{cases} 1 & t_2 \le u \le t_3 \\ 0 & \text{otherwise} \end{cases} = 1$$

$$N_{3,1} = \begin{cases} 1 & t_3 \le u \le t_4 \\ 0 & \text{otherwise} \end{cases} = 1$$

$$N_{4,1} = \begin{cases} 1 & t_4 \le u \le t_5 \\ 0 & \text{otherwise} \end{cases} = 1$$

$$N_{5,1} = \begin{cases} 1 & t_5 \le u \le t_6 \\ 0 & \text{otherwise} \end{cases} = 1$$

$$N_{6,1} = \begin{cases} 1 & t_6 \le u \le t_7 \\ 0 & \text{otherwise} \end{cases} = 1$$

Calculation for k=2

By using equation (3.30) recursive values are calculated. The values are as follows:

$N_{0,2} = 0$

$N_{1,2} = 0$

$N_{2,2} = (1-u)$

$N_{3,2} = u$

$N_{4,2} = 0$

$N_{5,2} = 0$

Calculation for k=3

$N_{0,3} = 0$

$N_{1,3} = (1-u)^2$

$N_{2,3} = 2u(1-u)$

$N_{3,3} = u^2$

$N_{4,3} = 0$

Calculation for k=4

$N_{0,4} = (1-u)^3$

$N_{1,4} = 3u(1-u)^2$

$N_{2,4} = 3u^2(1-u)$

$N_{3,4} = u^3$

Similarly getting all the values for 'k' in v direction by using equation (3.31) and substituting these values in equation (3.29)

$$\begin{aligned} Q(u,v) = {} & P_{00}(1-u)^3(1-v)^3 + P_{01}(1-u)^3 3v(1-v)^2 + P_{02}(1-u)^3 3v^2(1-v) + P_{03}(1-u)^3 v^3 + \\ & P_{10}3u(1-u)^2(1-v)^3 + P_{01}3u(1-u)^2 3v(1-v)^2 + P_{02}\,3u(1-u)^2\,3v^2(1-v) + P_{03}\,3u(1-u)^2\,v^3 + \\ & P_{20}3u^2(1-u)(1-v)^3 + P_{01}\,3u^2(1-u)\,3v(1-v)^2 + P_{02}\,3u^2(1-u)\,3v^2(1-v) + P_{03}\,3u^2(1-u)\,v^3 + \\ & P_{30}\,u^3(1-v)^3 + P_{01}\,u^3\,3v(1-v)^2 + P_{02}\,u^3\,3v^2(1-v) + P_{03}\,u^3\,v^3 \end{aligned} \quad (3.33)$$

Equation (3.33) represents the equation for the B-spline surface.

For verification of the algorithm, 4x4 control points are assumed. The control points are $P_{00}(1,1,2)$, $P_{01}(10,1,1.5)$, $P_{02}(20,1,2)$, $P_{03}(50,1,3)$, $P_{10}(1,12,1)$, $P_{11}(8,15,3)$, $P_{12}(30,20,1.5)$, $P_{13}(50,10,2)$, $P_{20}(1,25,0)$, $P_{21}(15,30,1)$, $P_{22}(25,30,3)$, $P_{23}(50,35,1)$, $P_{30}(1,50,2)$, $P_{31}(10,50,2)$, $P_{32}(20,50,1.5)$, $P_{33}(50,50,2)$

The assumed control points for the generation of B-spline surface using equation (3.33).

The surface is generated by making a program code in Matlab.

Matlab code for B-spline surface is as under:

```
clear all
close all
clc
tic
%Input Parameters (for x coordinate)
p0x=[1 10 20 50];
p1x=[1 8 30 50];
p2x=[1 15 25 50];
p3x=[1 10 20 50];
%Input Parameters (for y coordinate)
p0y=[1 1 1 1];
p1y=[12 15 20 10];
p2y=[25 30 35 35];
p3y=[50 50 50 50];
%Input Parameters (for z coordinate)
```

```
p0z=[2 1.5 2 3];
p1z=[1 3 1.5 2];
p2z=[0 1 3 1];
p3z=[2 2 1.5 2];
i=0;
for u=0.01:0.01:1
   i=i+1;
   j=0;
for v=0.01:0.01:1
   j=j+1;
%calculate final x coordinate
t1x=p0x(1)*power((1-u),3)*power((1-v),3);
t2x=p0x(2)*(power((1-u),3)*(3*v*(1-v)*(1-v)));
t3x=p0x(3)*(power((1-u),3)*(3*v*v*(1-v)));
t4x=p0x(4)*(power((1-u),3)*power((v),3));
t6x=p1x(1)*(power((1-v),3)*(3*u*(1-u)*(1-u)));
t7x=p1x(2)*(1-u)*(1-u)*(1-v)*(1-v)*9*u*v;
t8x=p1x(3)*(1-u)*(1-u)*(1-v)*9*u*v*v;
t9x=p1x(4)*(1-u)*(1-u)*power((v),3)*3*u;
t11x=p2x(1)*3*u*u*(1-u)*power((1-v),3);
t12x=p2x(2)*(1-u)*power((1-v),2)*9*u*u*v;
t13x=p2x(3)*(1-u)*power((1-v),1)*9*u*u*v*v;
t14x=p2x(4)*(1-u)*3*u*u*v*v*v;
t16x=p3x(1)*u*u*u*power((1-v),3);
t17x=p3x(2)*u*u*u*power((1-v),2)*3*v;
t18x=p3x(3)*u*u*u*power((1-v),1)*3*v*v;
t19x=p3x(4)*u*u*u*v*v*v;
tx(i,j)=t1x+t2x+t3x+t4x+t6x+t7x+t8x+t9x+t11x+t12x+t13x+t14x+t16x+t17x+t18x+t19x;
%calculate final y coordinate
t1y=p0y(1)*power((1-u),3)*power((1-v),3);
t2y=p0y(2)*(power((1-u),3)*(3*v*(1-v)*(1-v)));
t3y=p0y(3)*(power((1-u),3)*(3*v*v*(1-v)));
t4y=p0y(4)*(power((1-u),3)*power((v),3));
t6y=p1y(1)*(power((1-v),3)*(3*u*(1-u)*(1-u)));
t7y=p1y(2)*(1-u)*(1-u)*(1-v)*(1-v)*9*u*v;
t8y=p1y(3)*(1-u)*(1-u)*(1-v)*9*u*v*v;
t9y=p1y(4)*(1-u)*(1-u)*power((v),3)*3*u;
t11y=p2y(1)*3*u*u*(1-u)*power((1-v),3);
t12y=p2y(2)*(1-u)*power((1-v),2)*9*u*u*v;
t13y=p2y(3)*(1-u)*power((1-v),1)*9*u*u*v*v;
t14y=p2y(4)*(1-u)*3*u*u*v*v*v;
t16y=p3y(1)*u*u*u*power((1-v),3);
t17y=p3y(2)*u*u*u*power((1-v),2)*3*v;
t18y=p3y(3)*u*u*u*power((1-v),1)*3*v*v;
t19y=p3y(4)*u*u*u*v*v*v;
ty(i,j)=t1y+t2y+t3y+t4y+t6y+t7y+t8y+t9y+t11y+t12y+t13y+t14y+t16y+t17y+t18y+t19y;
%calculate final z coordinate
t1z=p0z(1)*power((1-u),3)*power((1-v),3);
t2z=p0z(2)*(power((1-u),3)*(3*v*(1-v)*(1-v)));
t3z=p0z(3)*(power((1-u),3)*(3*v*v*(1-v)));
t4z=p0z(4)*(power((1-u),3)*power((v),3));
t6z=p1z(1)*(power((1-v),3)*(3*u*(1-u)*(1-u)));
t7z=p1z(2)*(1-u)*(1-u)*(1-v)*(1-v)*9*u*v;
t8z=p1z(3)*(1-u)*(1-u)*(1-v)*9*u*v*v;
t9z=p1z(4)*(1-u)*(1-u)*power((v),3)*3*u;
t11z=p2z(1)*3*u*u*(1-u)*power((1-v),3);
t12z=p2z(2)*(1-u)*power((1-v),2)*9*u*u*v;
t13z=p2z(3)*(1-u)*power((1-v),1)*9*u*u*v*v;
t14z=p2z(4)*(1-u)*3*u*u*v*v*v;
t16z=p3z(1)*u*u*u*power((1-v),3);
t17z=p3z(2)*u*u*u*power((1-v),2)*3*v;
t18z=p3z(3)*u*u*u*power((1-v),1)*3*v*v;
t19z=p3z(4)*u*u*u*v*v*v;
tz(i,j)=t1z+t2z+t3z+t4z+t6z+t7z+t8z+t9z+t11z+t12z+t13z+t14z+t16z+t17z+t18z+t19z;
end
end
k=i;
```

```
r=j;
plot3(tx,ty,tz,'-r');
%plot(tx,tz,'-r');
hold on;
grid on;
%***************start to genearate text files and prift tool coordinates in
%respective file**********************
        x=fopen('tool_x.txt','wt');
        y=fopen('tool_y.txt','wt');
        z=fopen('tool_z.txt','wt');
        for i=1:1:k
           for j=1:1:r
              fprintf(x,'%10.5f\n',tx(i,j));
              fprintf(y,'%10.5f\n',ty(i,j));
              fprintf(z,'%10.5f\n',tz(i,j));
           end
        end
%***************end of genearate text files and prift tool coordinates in
%respective file**********************
for i=1:1:10
txf = fopen('mod_x.txt','r');
tx1 = fscanf(txf,'%15f',[i 1])';
tyf = fopen('mod_y.txt','r');
ty1 = fscanf(tyf,'%15f',[i 1])';
tzf = fopen('mod_z.txt','r');
tz1 = fscanf(tzf,'%15f',[i 1])';
 plot3(tx1,ty1,tz1,'-xb');
%plot(tx1,tz1,'xb');
end
toc;
```

3.4.1. Generated B-spline surface

After successful compilation of the program, the generated B-spline surface is shown in Fig. 3.6.

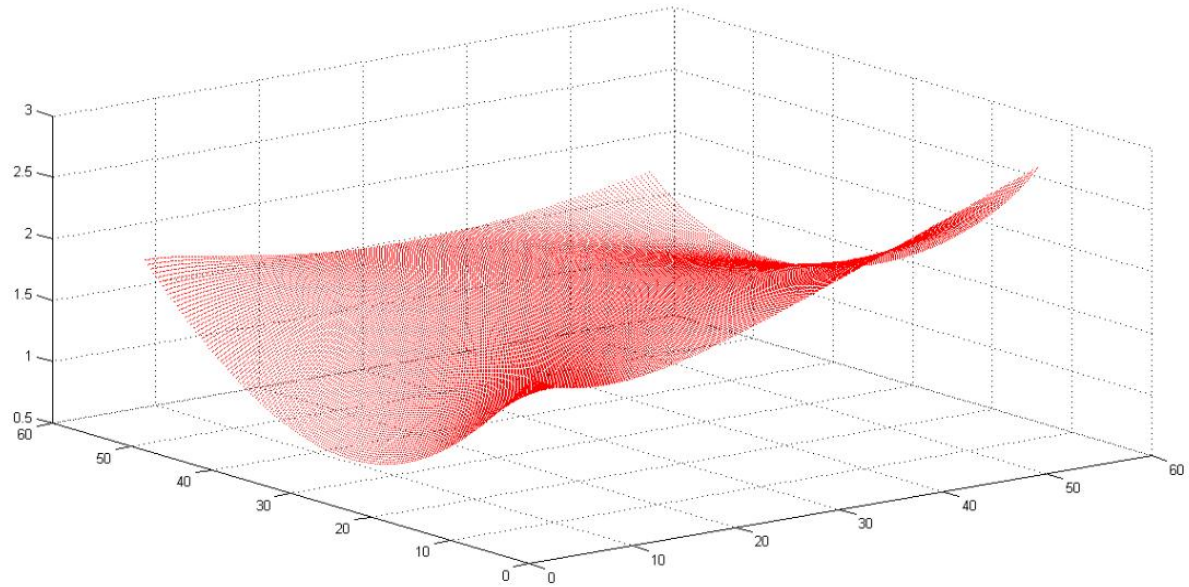

Fig. 3.6. Generated B-spline surface

To have a more clear visualization of the surface, the different views of the surface are given in Fig. 3.7 and 3.8.

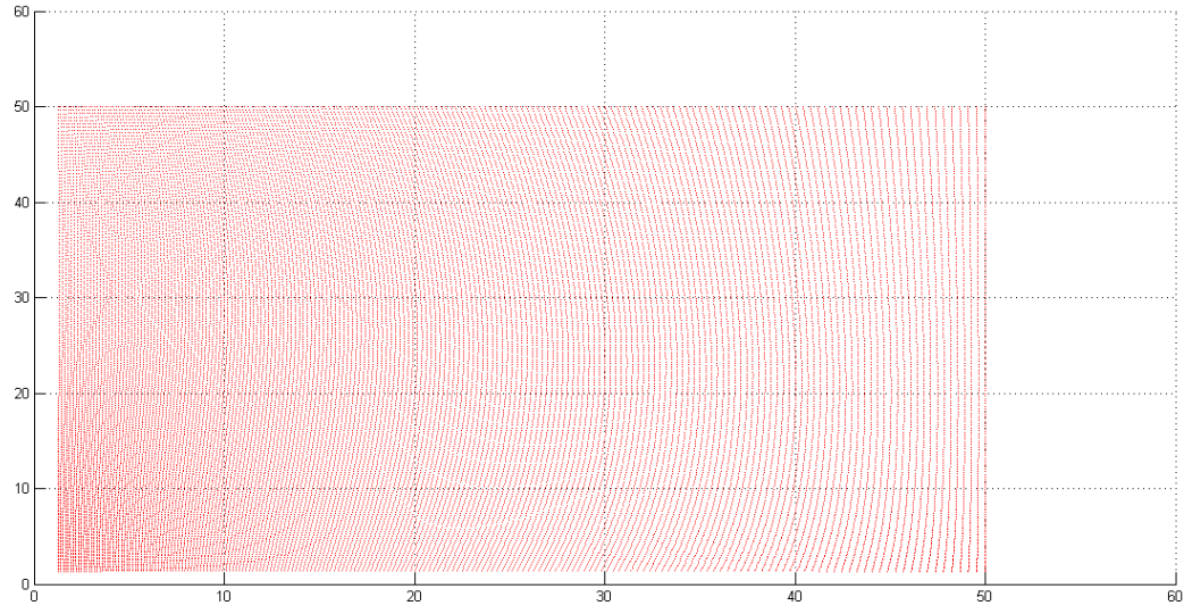

Fig. 3.7. X-Y view of B-spline surface

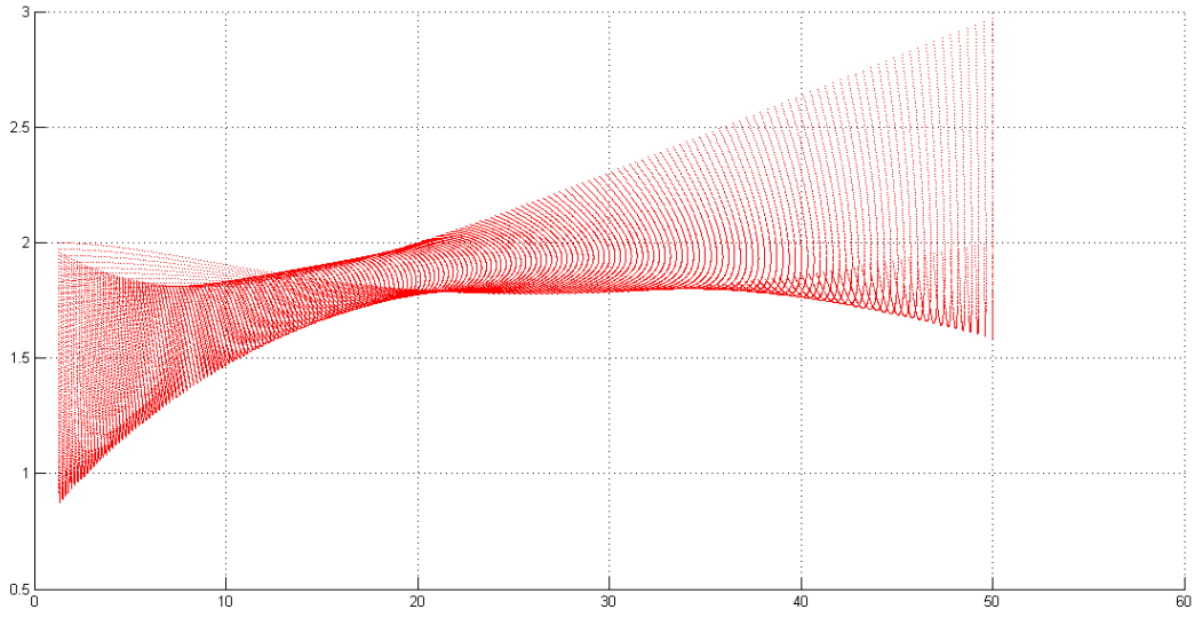

Fig. 3.8. X-Z view of B-spline surface

3.5 CALCULATION FOR THE FIRST POINT ON THE SURFACE

Now, as per the algorithm different points are generated on the surface for the tool path generation.

3.5.1 Determination of constants for surface coordinates

Constants as used in equation (3.4) are determined by fitting the data for u=0.01 and v varying from 0.01 to 1. The constants are $\alpha = 0.1,\ \beta = 0.6, \gamma = -3.95, \delta = 6$.

3.5.2 Determination of first coordinate on the surface

By using constants, the first coordinate on the B-spline surface is calculated at u = 0.01 and v= 0.01. The coordinates are calculated using eq. (3.5). These are:

$\hat{x}(0.01,0.01) = 1.27$

$\hat{y}(0.01,0.01) = 1.33$

$\hat{z}(0.01,0.01) = 1.96$

3.5.3 Determination of step size between two points on the surface

Step sizes between two consecutive points on the surface are determined analytically by using the software MATLAB, in which the curvature of the curve is predicted. For the maximum curvature, step size is minimum and for minimum curvature, step size between two consecutive point is more. The analytical prediction of step size is same as determined by Lartigue *et al.*[16]. The plots of abstraction of different points on the B-spline surface for the above example as shown below

Different break points for first tool path are plotted in Fig.3.9. These points are connected by cubic B-spline curve. The distance between two break points is called as **step size** whose value is varying from point to point.

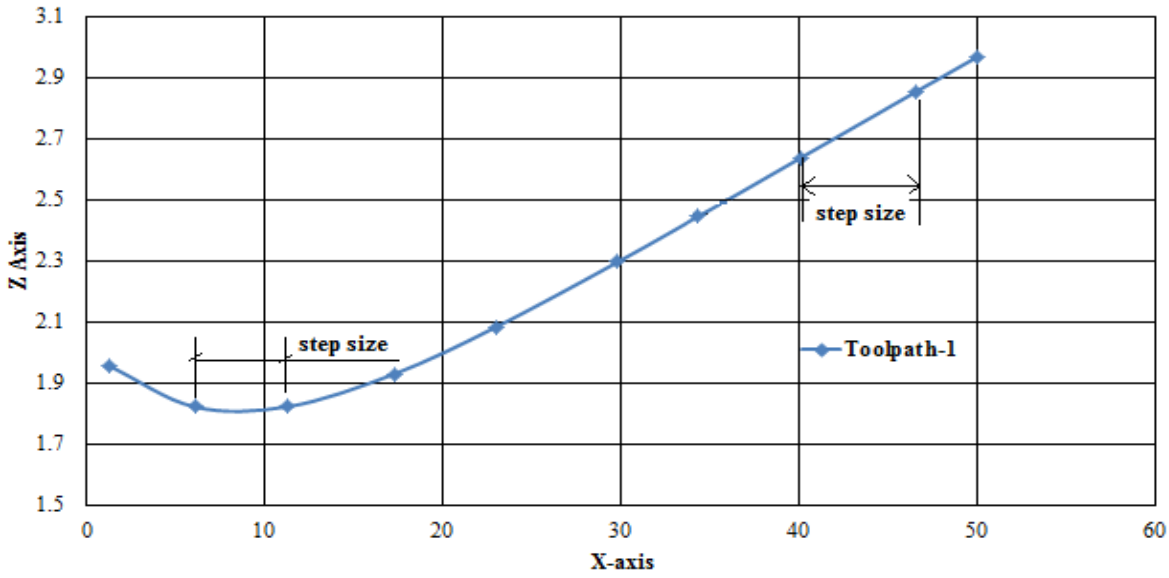

Fig. 3.9. Tool path 1 on B-spline surface

Different break points for second tool path are plotted in Fig.3.10. To determine the coordinates for toolpath 2, pick feed assumed from the literature review is approximately 1 mm.

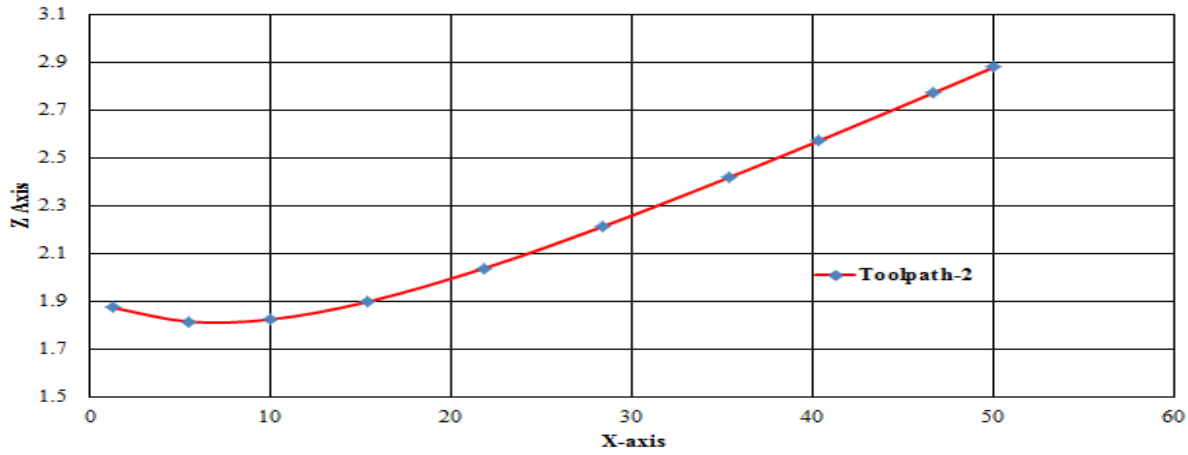

Fig. 3.10. Toolpath 2 on B-spline surface

Fig. 3.9 and 3.10 are combined in Fig. 3.11, which shows the variation in curvature of both the tool paths.

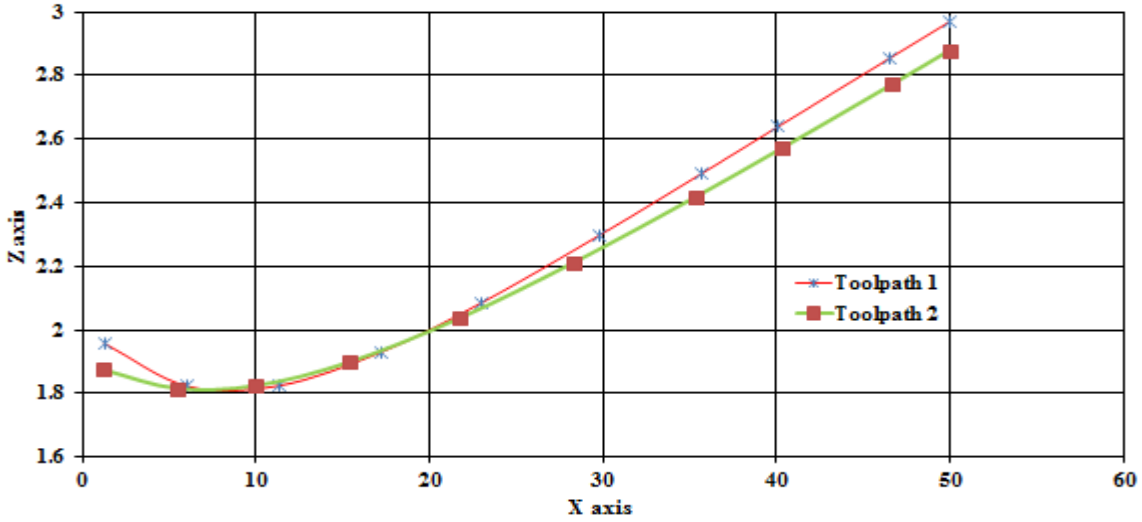

Fig. 3.11. Curvature of toolpath 1 and 2 on B-spline surface

3.5.4 Determination of maximum scallop height

The pick feed, which is the path interval, is determined such that the maximum scallop height along the scallop curve is within the prescribed tolerance. The scallop curve is an intersection curve between the two consecutive toolpaths. The resultant scallop height is measured as the perpendicular distance from the second toolpath coordinates to the first toolpath. For the different locations on the scallop curve scallop heights are plotted in Fig. 3.12. To select the

pick feed, the value of maximum scallop height is selected. In the present study, the value of scallop height is selected as 0.08 mm. For the chosen value of scallop height, the approximate value of pick feed is 1 mm as assumed previously.

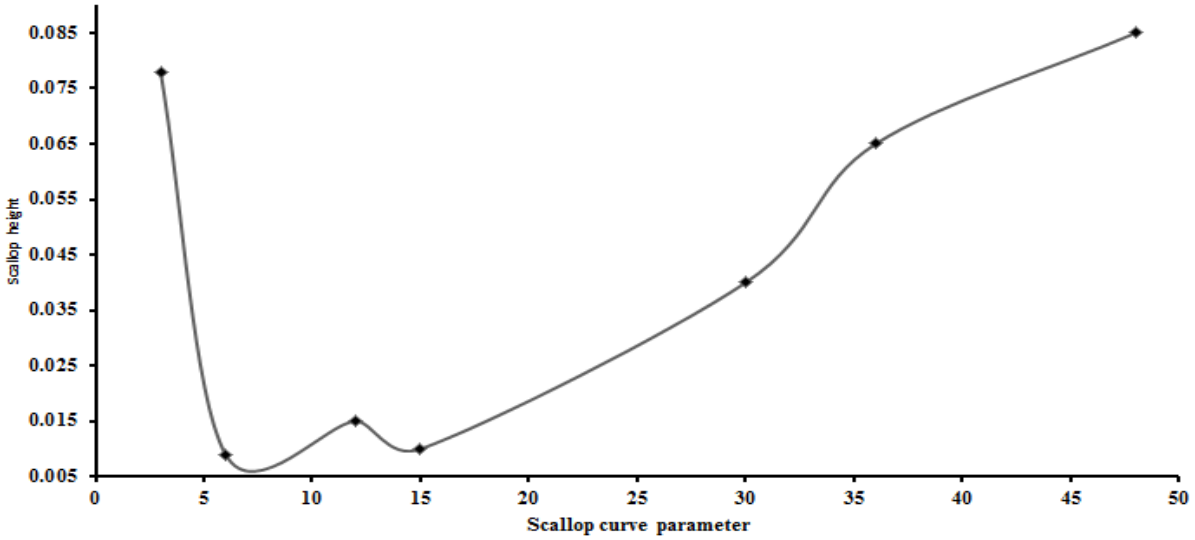

Fig. 3.12. Graphical representation for Scallop height at different cutter location

3.5.5 Graphical presentation of break points on different toolpaths

After calculating the value of scallop height and pick feed all the coordinates generated on the B-spline surface are plotted, as shown in Fig.3.13.

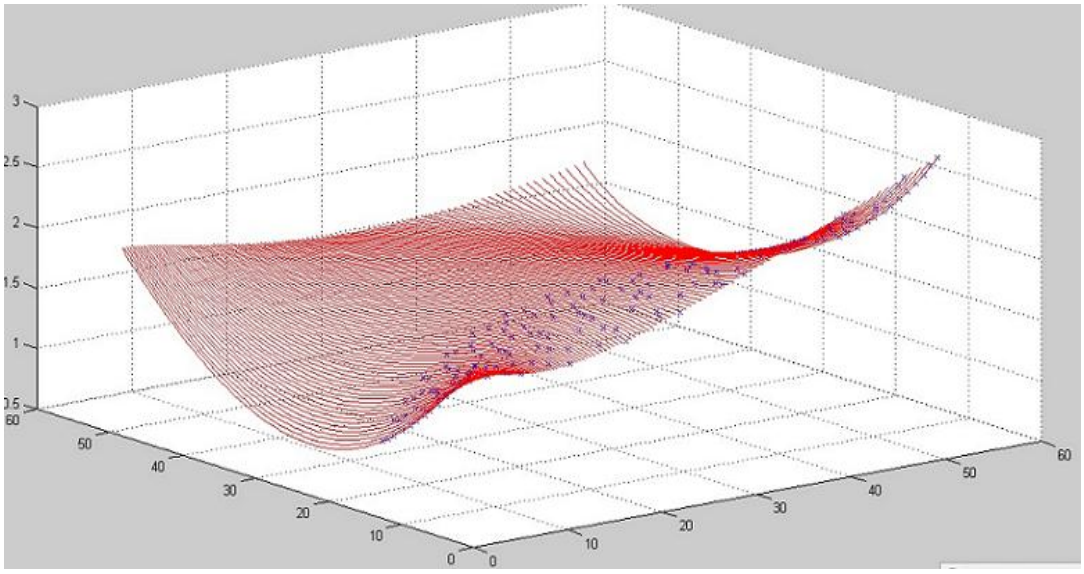

Fig. 3.13. Breakpoints for different toolpaths on the surface

To have a more clear view of points on the surface, the different orientation of the surface is given in Fig. 3.14 and 3.15.

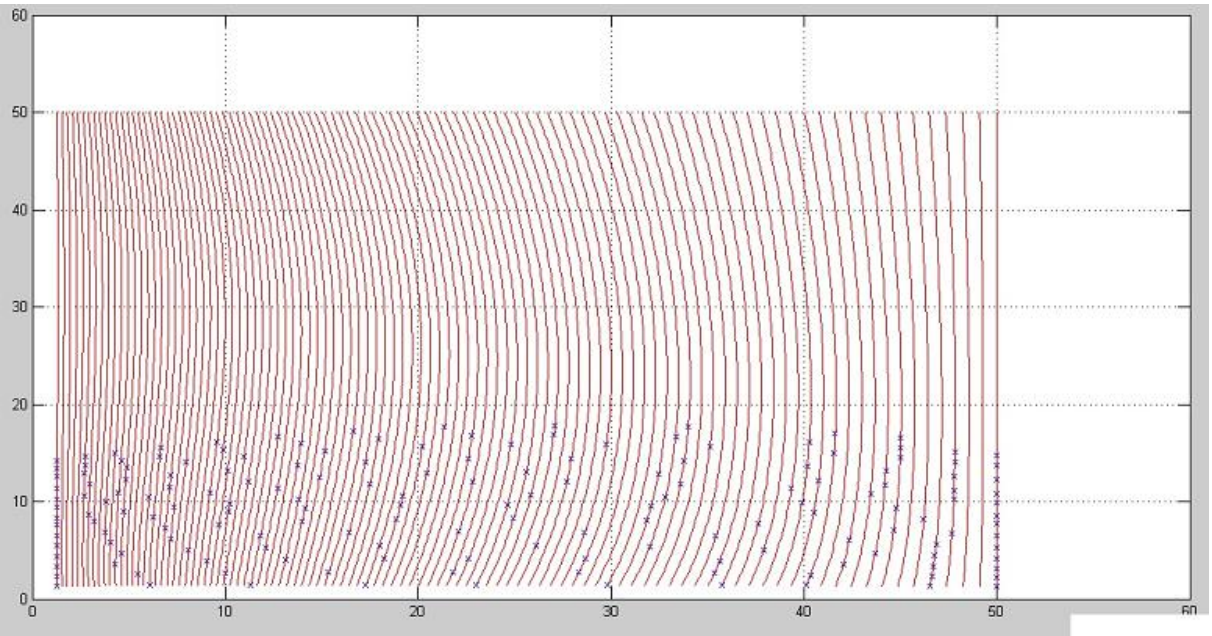

Fig. 3.14. X-Y view of break-points on the surface

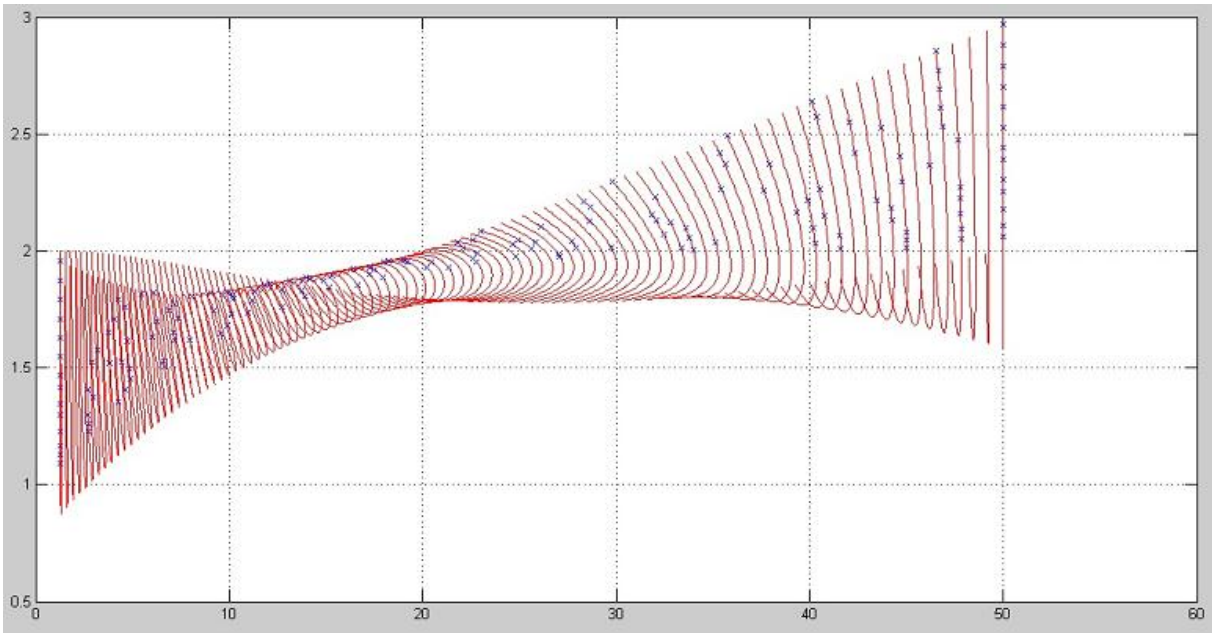

Fig. 3.15 X-Z view of break-points on the surface

The surface generated in the current chapter is used for making of the surface on a vertical CNC milling machine.

CHAPTER 4
EXPERIMENTAL SETUP

Coordinates for B-spline surface generated using the program code in Matlab, as discussed in previous chapter, are used to machine the surface on the mild steel work piece using 3-axis vertical CNC milling machine with a ball-end mill cutter.

4.1 EXPERIMENTAL SETUP

The surface coordinates generated by Matlab were used to write a program code using word address format[18] on a vertical CNC milling machine shown in Fig. 4.1.

Fig. 4.1 Vertical CNC Milling Machine

For the machining of the surface, a ball end-mill cutter of diameter 8 mm has been used. The surface is generated on a billet of size 100x100x20 mm^3. The program code is given in section 4.2. The experimental setup is shown in Fig. 4.2.

Fig. 4.2 Experimental setup of Vertical CNC milling machine

4.2 TOOLPATH GENERATION CODE FOR MACHINING

```
;%_N_HSM_LIN_TARGET_PIT
;$PATH=/_N_PIT_DIR
N1 ; PART NAME      : 3331
N2 ; PROGRAM NUMBER : 5000
N3 ; DATE - TIME    : 12-JUL-2012 - 17:00:15
N4 ; TOOLS USED     :
N5 ; - T2  BALL NOSE MILL DIAMETER = 8. CORNER RADIUS = 4.
N6 ; - LENGTH OUT OF HOLDER = 60.
N7 G17 G90 G40
N8 TRANS
N9 SOFT
N10 CFIN
N11 FGROUP (X,Y,Z)
N12 G54
N13 G90 G40 G17
N14 T2
N15 M6
N16 G90 G54
N17 M1
N18 G0 Z50.
N19 S1000 M3
N20 MSG("HSM-LIN-TARGET - HSM-RASTER")
N21 G0 X0 Y0
N22 G0 Z10.
N23 M8
N24 G642
N25 G00 X1.27 Y1.33 Z10
N26 G1   X1.27          Y1.33          Z1.96  F250
N27 G1   X6.07          Y1.38          Z1.82
N28 G1   X11.32         Y1.42          Z1.82
N29 G1   X17.27         Y1.45          Z1.93
N30 G1   X23.01         Y1.45     Z2.09
N31 G1   X29.82         Y1.43          Z2.30
N32 G1   X35.74         Y1.39          Z2.49
N33 G1   X40.11         Y1.36          Z2.64
```

```
N34 G1  X46.53      Y1.31       Z2.85
N35 G1  X50         Y1.27       Z2.97
N36 G1  X50   Y1.27  Z10
N37 G1  X50   Y2.16
N38 G1  X50   Y2.16  Z2.88
N39 G1  X46.62      Y2.28       Z2.77
N40 G1  X40.34      Y2.48       Z2.57
N41 G1  X35.34      Y2.62       Z2.42
N42 G1  X28.35      Y2.75       Z2.21
N43 G1  X21.79      Y2.80       Z2.04
N44 G1  X15.36      Y2.76       Z1.90
N45 G1  X10.00      Y2.66       Z1.82
N46 G1  X5.48       Y2.51       Z1.82
N47 G1  X1.26       Y2.34       Z1.87
N48 G1          Z10
N49 G1  X1.26       Y3.36   Z10
N50 G1  X1.26       Y3.36       Z1.79
N51 G1  X4.31       Y3.57       Z1.79
N52 G1  X9.06       Y3.86       Z1.82
N53 G1  X13.11      Y4.03       Z1.87
N54 G1  X18.22      Y4.14       Z1.96
N55 G1  X22.60      Y4.16       Z2.05
N56 G1  X28.66      Y4.08       Z2.19
N57 G1  X35.61      Y3.87       Z2.37
N58 G1  X42.03      Y3.58       Z2.55
N59 G1  X46.70      Y3.32       Z2.69
N60 G1  X50         Y3.12       Z2.79
N61 G1          Z10
N62 G1   X50       Y4.15       Z10
N63 G1   X50       Y4.15       Z2.7
N64 G1  X46.78      Y4.43       Z2.61
N65 G1  X43.69      Y4.67       Z2.52
N66 G1  X37.90      Y5.05       Z2.37
N67 G1  X31.99      Y5.33       Z2.23
N68 G1  X26.09      Y5.50       Z2.10
N69 G1  X17.99      Y5.49       Z1.95
N71 G1  X12.09      Y5.27       Z1.86
N72 G1  X8.11       Y5.02       Z1.80
N73 G1  X4.61       Y4.72       Z1.76
N74 G1  X1.26       Y4.40       Z1.71
N75 G1          Z10
N76 G1  X1.26       Y5.45       Z10
N77 G1  X1.26       Y5.45       Z1.63
N78 G1  X4.04       Y5.79       Z1.71
N79 G1  X7.16       Y6.14       Z1.77
N80 G1  X11.84      Y6.54       Z1.86
N81 G1  X16.40      Y6.79   Z1.93
N82 G1  X22.10      Y6.91       Z2.01
N83 G1  X28.63      Y6.83       Z2.13
N84 G1  X35.43      Y6.52       Z2.26
N85 G1  X42.34      Y6.01       Z2.42
N86 G1  X46.84      Y5.60       Z2.53
N87 G1  X50         Y5.26       Z2.61
N88 G1          z10
N89 G1  X50         Y6.44       Z10
N90 G1  X50         Y6.44       Z2.53
N91 G1  X47.67      Y6.73       Z2.47
N92 G1  X44.66      Y7.08   Z2.40
```

```
N93 G1  X37.62        Y7.73    Z2.26
N94 G1  X31.85        Y8.09    Z2.16
N95 G1  X24.95        Y8.30    Z2.05
N96 G1  X18.88        Y8.23        Z1.96
N97 G1  X13.99        Y7.99    Z1.89
N98 G1  X9.69         Y7.62    Z1.81
N99 G1  X6.89         Y7.31    Z1.75
N100 G1  X3.76        Y6.89    Z1.65
N101 G1  X1.26        Y6.51    Z1.55
N102 G1             Z10
N103 G1  X1.26        Y7.60        Z10
N104 G1  X1.26        Y7.60        Z1.47
N105 G1  X3.20        Y7.94        Z1.57
N106 G1  X6.29        Y8.43        Z1.70
N107 G1  X10.16 Y8.9    Z1.80
N108 G1  X14.14 Y9.32   Z1.88
N109 G1  X19.08 Y9.61   Z1.96
N110 G1  X24.63 Y9.70   Z2.03
N111 G1  X32.06 Y9.49   Z2.13
N112 G1  X40.49 Y8.85   Z2.26
N113 G1  X46.21 Y8.20   Z2.37
N114 G1  X50          Y7.68        Z2.44
N115 G1             Z10
N116 G1  X50          Y8.55        Z10
N117 G1  X50          Y8.55        Z2.39
N118 G1  X44.79 Y9.28   Z2.30
N119 G1  X39.89 Y9.84   Z2.22
N120 G1  X32.80 Y10.40           Z2.11
N121 G1  X25.85 Y10.64           Z2.03
N122 G1  X19.20 Y10.53           Z1.95
N123 G1  X13.82 Y10.17           Z1.87
N124 G1  X10.23 Y9.79   Z1.79
N125 G1  X7.34        Y9.40        Z1.71
N126 G1  X4.72        Y8.98        Z1.61
N127 G1  X2.92        Y8.65        Z1.52
N128 G1  X1.26        Y8.34        Z1.42
N129 G1             Z10
N130 G1  X1.26        Y9.46        Z10
N131 G1  X1.26        Y9.46        Z1.34
N132 G1  X3.84        Y9.99        Z1.52
N133 G1  X6.06        Y10.41       Z1.63
N134 G1  X9.20        Y10.92       Z1.75
N135 G1  X12.70 Y11.38           Z1.84
N136 G1  X17.48 Y11.81           Z1.92
N137 G1  X22.85 Y12.04           Z1.99
N138 G1  X27.69 Y12.04           Z2.04
N139 G1  X33.57 Y11.80           Z2.10
N140 G1  X39.34 Y11.32           Z2.16
N141 G1  X43.44 Y10.85   Z2.21
N142 G1  X47.76 Y10.24           Z2.27
N143 G1  X50   Y9.89    Z2.31
N144 G1             Z10
N145 G1
N146 G1  X50          Y10.81       Z10
N147 G1  X50          Y10.81       Z2.26
N148 G1  X47.78 Y11.17           Z2.23
N149 G1  X44.19 Y11.70           Z2.18
N150 G1  X40.75 Y12.13           Z2.15
```

```
N151 G1  X32.45 Y12.83          Z2.07
N152 G1  X25.59 Y13.02          Z2.01
N153 G1  X20.44 Y12.90          Z1.95
N154 G1  X14.90 Y12.49          Z1.87
N155 G1  X11.18 Y12.06          Z1.79
N156 G1  X7.11          Y11.42  Z1.65
N157 G1  X4.48          Y10.92  Z1.52
N158 G1  X2.67          Y10.53  Z1.41
N159 G1  X1.27          Y10.22  Z1.30
N160 G1                 Z10
N161 G1  X1.27          Y11.39  Z10
N162 G1  X1.27          Y11.39  Z1.23
N163 G1  X2.99          Y11.79  Z1.38
N164 G1  X4.84          Y12.21  Z1.49
N165 G1  X7.19          Y12.68  Z1.62
N166 G1  X10.11 Y13.20          Z1.73
N167 G1  X13.74 Y13.71          Z1.83
N168 G1  X17.26 Y14.08          Z1.89
N169 G1  X22.59 Y14.39          Z1.97
N170 G1  X27.94 Y14.44          Z2.02
N171 G1  X33.79 Y14.21          Z2.06
N172 G1  X40.17 Y13.66          Z2.09
N173 G1  X44.25 Y13.15          Z2.13
N174 G1  X47.80 Y12.61          Z2.16
N175 G1  X50            Y12.23  Z2.18
N176 G1                 Z10
N177 G1  X50            Y13.70  Z10
N178 G1  X50            Y13.70  Z2.10
N179 G1  X47.82 Y14.08          Z2.09
N180 G1  X44.99 Y14.52          Z2.08
N181 G1  X41.57 Y14.98          Z2.06
N182 G1  X35.12 Y15.60          Z2.03
N183 G1  X29.76 Y15.86          Z2.01
N184 G1  X24.79 Y15.88          Z1.97
N185 G1  X20.22 Y15.69          Z1.92
N186 G1  X15.14 Y15.22          Z1.84
N187 G1  X10.99 Y14.64          Z1.73
N188 G1  X7.97          Y14.10  Z1.62
N189 G1  X4.89          Y13.45  Z1.45
N190 G1  X2.72          Y12.93  Z1.29
N191 G1  X1.28          Y12.57  Z1.16
N192 G1                 Z10
N193 G1  X1.28          Y13.38  Z10
N194 G1  X1.28          Y13.38  Z1.13
N195 G1  X2.73          Y13.76  Z1.26
N196 G1  X4.60          Y14.22  Z1.40
N197 G1  X6.61          Y14.68  Z1.52
N198 G1  X9.88          Y15.34  Z1.67
N199 G1  X13.92 Y15.98          Z1.80
N200 G1  X17.92 Y16.44          Z1.88
N201 G1  X22.79 Y16.78          Z1.95
N202 G1  X27.02 Y16.88          Z1.98
N203 G1  X33.34 Y16.71          Z2.01
N204 G1  X40.27 Y16.13          Z2.03
N205 G1  X45.00 Y15.53          Z2.04
N206 G1  X47.83 Y15.08          Z2.05
N207 G1  X50            Y14.70  Z2.05
N208 G1                 Z10
```

```
N209 G1  X50          Y15.72      Z10
N210 G1  X50          Y15.72      Z2.01
N211 G1  X47.83 Y16.10            Z2.01
N212 G1  X45.02 Y16.54            Z2.01
N213 G1  X41.62 Y16.99            Z2.01
N214 G1  X33.99 Y17.67            Z2.00
N215 G1  X27.08 Y17.85            Z1.97
N216 G1  X21.35 Y17.65            Z1.92
N217 G1  X16.61 Y17.23            Z1.85
N218 G1  X12.73 Y16.70            Z1.75
N219 G1  X9.56        Y16.15      Z1.64
N220 G1  X6.65        Y15.54      Z1.50
N221 G1  X4.30        Y14.99      Z1.35
N222 G1  X2.74        Y14.59      Z1.22
N223 G1  X1.28        Y14.20      Z1.08
N224 G1          Z10
N225 G1  X1.28        Y15.45      Z10
N226 G1  X1.28        Y15.45      Z1.03
N227 G1  X2.77        Y15.86      Z1.18
N228 G1  X4.67        Y16.36      Z1.33
N229 G1  X6.36        Y16.78      Z1.45
N230 G1  X8.51        Y17.26      Z1.56
N231 G1  X12.00 Y17.94            Z1.71
N232 G1  X16.71 Y18.63            Z1.84
N233 G1  X21.43 Y19.08            Z1.91
N234 G1  X27.16 Y19.32            Z1.96
N235 G1  X31.09 Y19.29            Z1.97
N236 G1  X35.26 Y19.10 Z1.98
N237 G1  X38.39 Y18.86            Z1.97
N238 G1  X42.99 Y18.36            Z1.97
N239 G1  X45.03 Y18.08            Z1.96
N240 G1  X47.84 Y17.65            Z1.95
N241 G1  X50    Y17.28 Z1.94
N242 G1          Z10
N243 G1  X50    Y18.34 Z10
N244 G1  X50    Y18.34 Z1.90
N245 G1  X47.13 Y18.82            Z1.92
N246 G1  X44.35 Y19.22            Z1.93
N247 G1  X39.05 Y19.83            Z1.95
N248 G1  X31.12 Y20.28            Z1.96
N249 G1  X25.05 Y20.24            Z1.94
N250 G1  X19.07 Y19.84            Z1.87
N251 G1  X14.99 Y19.34            Z1.78
N252 G1  X11.65 Y18.79            Z1.68
N253 G1  X8.56        Y18.16      Z1.54
N254 G1  X6.06        Y17.58      Z1.40
N255 G1  X4.38        Y17.16      Z1.28
N256 G1  X2.48        Y16.64      Z1.12
N257 G1  X1.29        Y16.31      Z1.00
N258 G1          Z10
N259 G1  X1.29        Y17.17      Z10
N260 G1  X1.29        Y17.17      Z0.98
N261 G1  X2.81        Y17.61      Z1.12
N262 G1  X4.41        Y18.04  Z1.26
N263 G1  X6.44        Y18.57      Z1.40
N264 G1  X8.60        Y19.07      Z1.53
N265 G1  X11.30 Y19.64            Z1.65
N266 G1  X13.34 Y20.00            Z1.72
```

```
N267 G1  X17.72 Y20.64          Z1.83
N268 G1  X23.02 Y21.12          Z1.91
N269 G1  X30.00         Y21.30      Z1.95
N270 G1  X37.78 Y20.96 Z1.94
N271 G1  X43.67 Y20.36          Z1.91
N272 G1  X47.13 Y19.88          Z1.89
N273 G1  X50    Y19.41 Z1.86
N274 G1             Z10
N275 G1  X50    Y21.04 Z10
N276 G1  X50    Y21.04 Z1.81
N277 G1  X49.27 Y21.16          Z1.82
N278 G1  X48.55 Y21.27          Z1.83
N279 G1  X45.73 Y21.68          Z1.86
N280 G1  X42.32 Y22.10          Z1.89
N281 G1  X35.30 Y22.66          Z1.93
N282 G1  X27.79 Y22.78          Z1.93
N283 G1  X22.56 Y22.54          Z1.90
N284 G1  X16.87 Y21.95          Z1.80
N285 G1  X11.76 Y21.11          Z1.64
N286 G1  X7.93          Y20.29      Z1.46
N287 G1  X5.12          Y19.58      Z1.28
N288 G1  X2.83          Y18.95      Z1.09
N289 G1  X1.30          Y18.51      Z0.94
N290 G1             Z10
N291 G1  X1.30          Y19.41      Z10
N292 G1  X1.30          Y19.41      Z0.92
N293 G1  X3.82          Y20.14      Z1.15
N294 G1  X5.49          Y20.59      Z1.28
N295 G1  X7.97          Y21.22      Z1.44
N296 G1  X11.01 Y21.89          Z1.59
N297 G1  X13.86 Y22.44          Z1.70
N298 G1  X17.80 Y23.03          Z1.81
N299 G1  X22.08 Y23.48          Z1.88
N300 G1  X26.72 Y23.75          Z1.92
N301 G1  X31.73 Y23.80          Z1.93
N302 G1  X42.32 Y23.16          Z1.87
N303 G1  X45.72 Y22.76          Z1.83
N304 G1  X50    Y22.14 Z1.78
N305 G1             Z10
N306 G1  X50    Y23.25 Z10
N307 G1  X50    Y23.25 Z1.75
N308 G1  X48.54 Y23.46          Z1.77
N308 G1  X46.41 Y23.75          Z1.80
N310 G1  X42.97 Y24.15          Z1.84
N312 G1  X37.76 Y24.59          Z1.89
N313 G1  X31.72 Y24.81          Z1.92
N314 G1  X25.66 Y24.70          Z1.91
N315 G1  X20.63 Y24.33          Z1.85
N316 G1  X15.16 Y23.61          Z1.73
N317 G1  X11.44 Y22.92          Z1.60
N318 G1  X8.74          Y22.33      Z1.47
N319 G1  X6.21          Y21.71      Z1.31
N320 G1  X4.17          Y21.16      Z1.16
N321 G1  X2.55          Y20.70      Z1.02
N322 G1  X1.30          Y20.34      Z0.90
N323 G1             Z10
N324 G1  X1.30          Y21.27      Z10
N325 G1  X1.30          Y21.27      Z0.89
```

```
N326 G1  X2.88          Y21.73      Z1.04
N327 G1  X4.86          Y22.29      Z1.20
N328 G1  X8.04          Y23.11      Z1.41
N329 G1  X12.27 Y24.04              Z1.62
N330 G1  X17.84 Y24.97              Z1.79
N331 G1  X24.10 Y25.60              Z1.89
N332 G1  X32.87 Y25.82              Z1.91
N333 G1  X39.65 Y25.51              Z1.86
N334 G1  X44.32 Y25.08              Z1.80
N335 G1  X47.82 Y24.66              Z1.75
N336 G1  X50    Y24.36 Z1.72
N337 G1            Z10
N338 G1  X50    Y25.48 Z10
N339 G1  X50    Y25.48 Z1.69
N340 G1  X47.81 Y25.77              Z1.73
N341 G1  X44.99 Y26.10              Z1.78
N342 G1  X41.59 Y26.42              Z1.82
N343 G1  X34.02 Y26.82              Z1.89
N344 G1  X26.16 Y26.72              Z1.90
N345 G1  X19.69 Y26.18              Z1.82
N346 G1  X15.20 Y25.54              Z1.71
N347 G1  X10.71 Y24.68              Z1.54
N348 G1  X6.98          Y23.80      Z1.33
N349 G1  X4.21          Y23.06      Z1.14
N350 G1  X2.57          Y22.60      Z1.00
N351 G1  X1.31          Y22.23      Z0.88
N352 G1          Z10
N353 G1  X1.31          Y23.20      Z10
N354 G1  X1.31          Y23.20      Z0.87
N355 G1  X2.91          Y23.67      Z1.02
N356 G1  X5.25          Y24.32      Z1.20
N357 G1  X8.46          Y25.14      Z1.41
N358 G1  X11.12 Y25.74              Z1.55
N359 G1  X16.95 Y26.80              Z1.75
N360 G1  X23.56 Y27.55 Z1.87
N361 G1  X31.07 Y27.86              Z1.90
N362 G1  X38.31 Y27.70              Z1.85
N363 G1  X42.91 Y27.38              Z1.79
N364 G1  X47.08 Y26.96              Z1.72
N365 G1  X50    Y26.60 Z1.67
N366 G1          Z10
N367 G1  X50    Y27.73 Z10
N368 G1  X50    Y27.73 Z1.65
N369 G1  X47.79 Y27.99              Z1.69
N370 G1  X44.95 Y28.28              Z1.74
N371 G1  X40.87 Y28.60              Z1.81
N372 G1  X34.54 Y28.87              Z1.87
N373 G1  X26.62 Y28.75              Z1.89
N374 G1  X19.66 Y28.15              Z1.81
N375 G1  X13.53 Y27.21              Z1.64
N376 G1  X8.47          Y26.12      Z1.40
N377 G1  X5.27          Y25.31      Z1.20
N378 G1  X2.92          Y24.66      Z1.01
N379 G1  X1.31          Y24.20      Z0.87
N380 G1          Z10
N381 G1  X1.31          Y25.21      z10
N382 G1  X1.31          Y25.21      Z0.87
N383 G1  X2.93          Y25.66      Z1.01
```

```
N384 G1  X4.94          Y26.22      Z1.17
N385 G1  X7.76          Y26.94      Z1.35
N386 G1  X11.14 Y27.72              Z1.53
N387 G1  X16.06 Y28.64              Z1.71
N388 G1  X22.01 Y29.41              Z1.84
N389 G1  X8.73          Y29.85      Z1.88
N390 G1  X35.10 Y29.89              Z1.86
N391 G1  X42.84 Y29.54              Z1.76
N392 G1  X46.34 Y29.24              Z1.70
N393 G1  X48.51 Y29.02              Z1.66
N394 G1  X50            Y28.86      Z1.63
N395 G1             Z2
N396 G1  G28 X0 Y0
N397 G1  M30
%
```

CHAPTER 5
RESULTS AND DISCUSSIONS

Different break points for first tool path, plotted in Fig.3.9 were connected by cubic B-spline curve having 9 piecewise cubic polynomial segments (10 control points). Different break points for first tool path are also plotted with linear segments, as shown in Fig. 5.1.

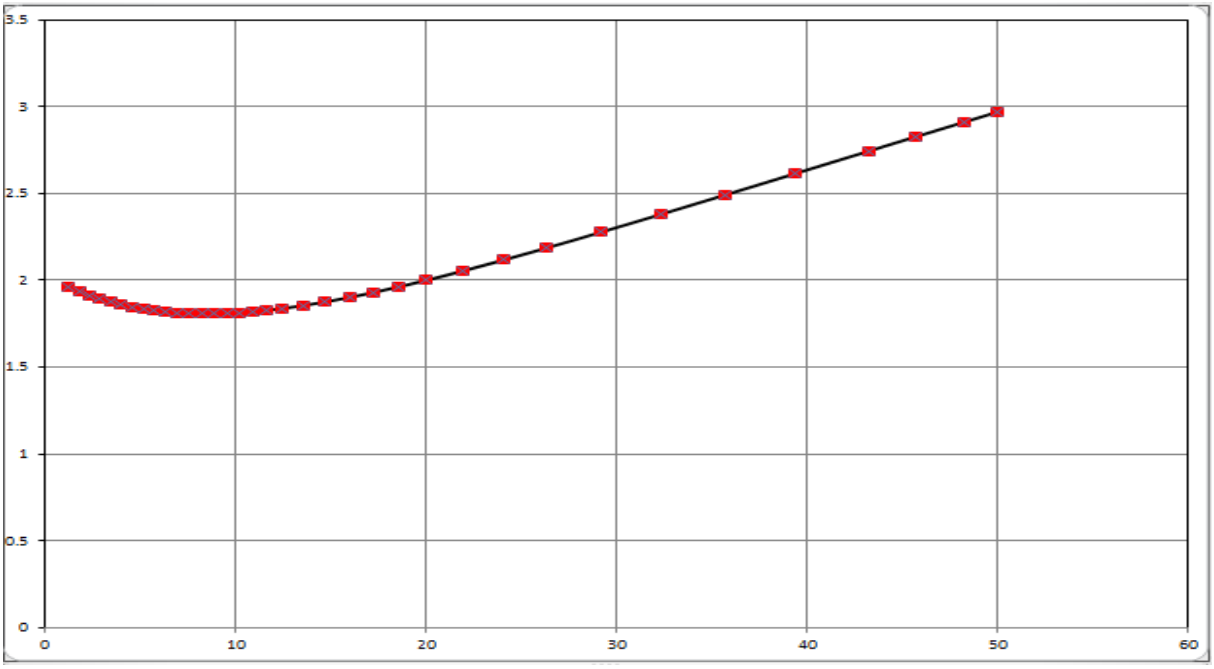

Fig. 5.1. Tool path represented by linear segment

It is found that for having the accurate shape of the curve 35 linear segments are needed. Thus the number of segments has been reduced by 74% with the use of the algorithm. The difference of the number of segments required becomes significant when the tool path is long and has many regions with high curvature.

The program code written in word address format, as given in section 4.2 is run on the CNC vertical milling machine, shown in Fig. 4.1. The surface generated on CNC machine is shown in Fig. 5.2.

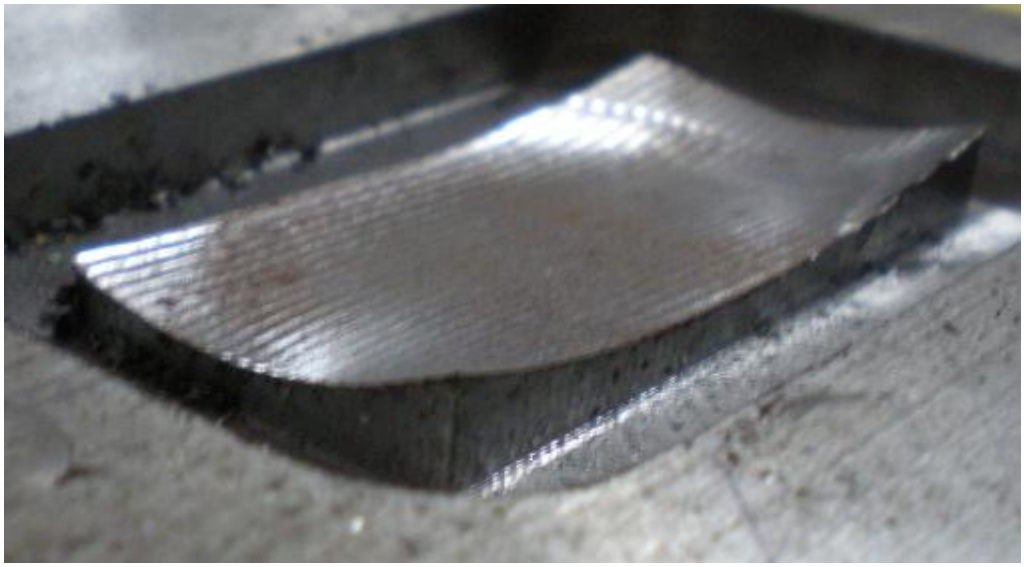

Fig. 5.2. Profile generated on machine

For comparing the required and generated surfaces, the two surfaces are to be overlapped. For comparison, coordinates of generated surface on MATLAB are imported into Pro-E as shown in Fig. 5.3.

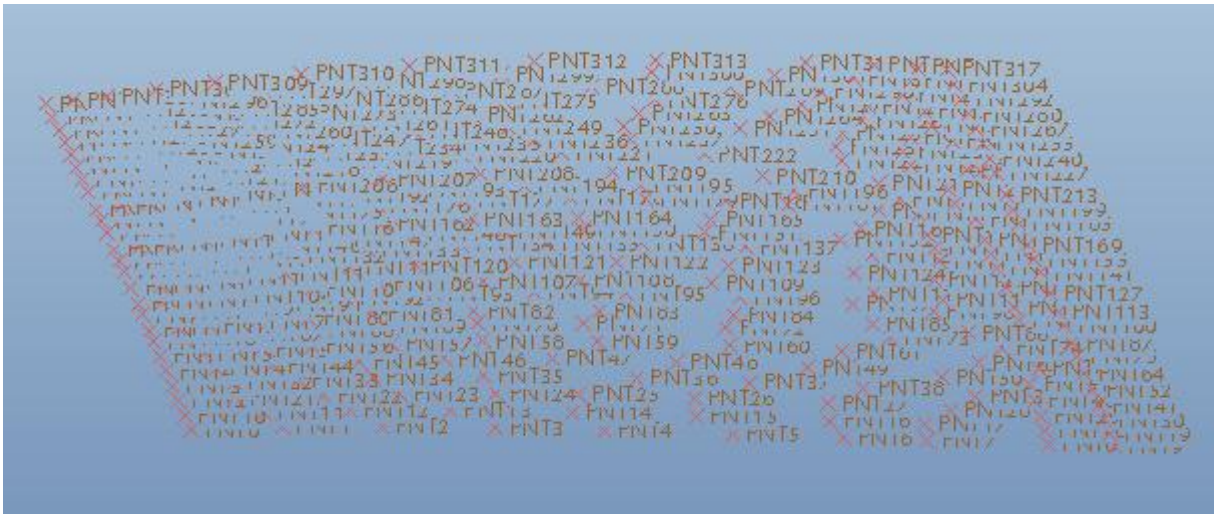

Fig. 5.3. Coordinates imported into Pro-E

By joining these points through Spline curve in Pro-E, free form surface is generated as shown in Fig. 5.4.

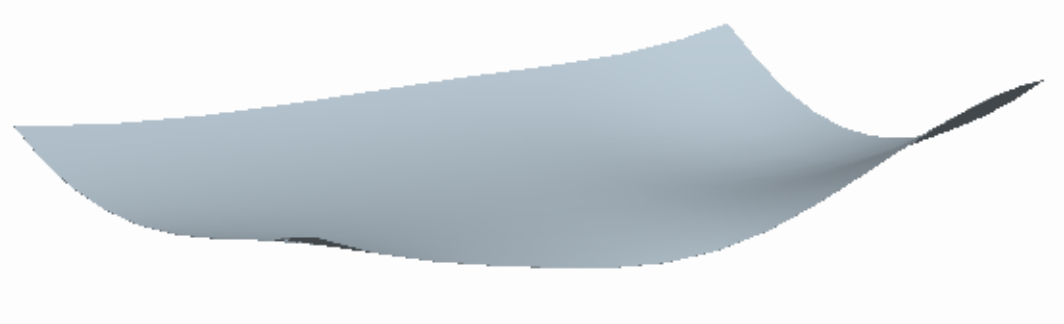

Fig. 5.4 Profile generated in Pro-E

The coordinates of surface generated on steel workpiece are measured using Coordinate Measuring Machine (CMM) as shown in Fig. 5.5. Thereafter these coordinates are also imported into Pro-E as shown in Fig. 5.6.

Fig 5.5 Coordinates Measuring Machine

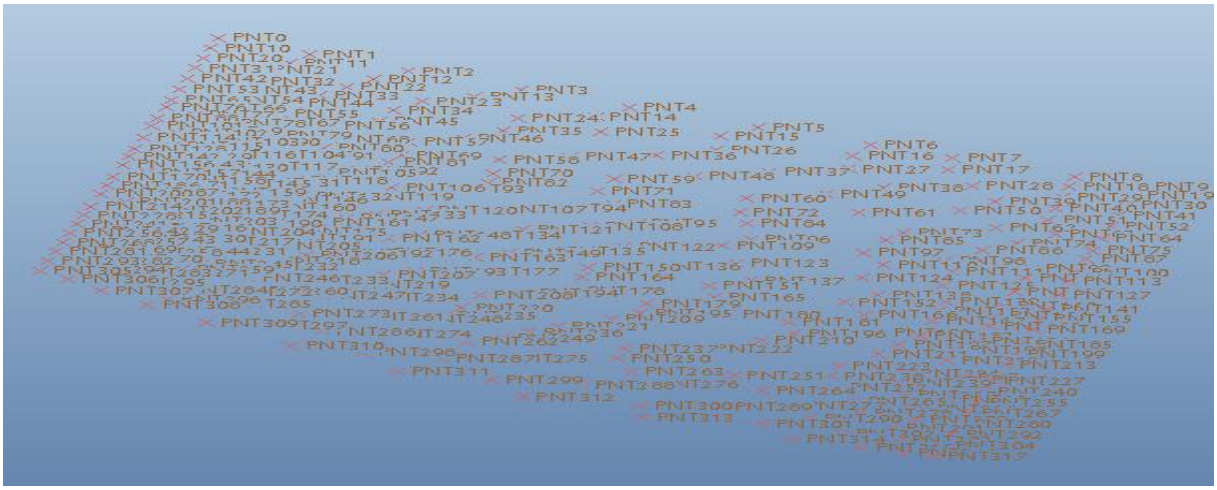

Fig. 5.6 Coordinates imported into Pro-E

By joining these points through Spline curve in Pro-E, another free form surface is generated as shown in Fig. 5.7.

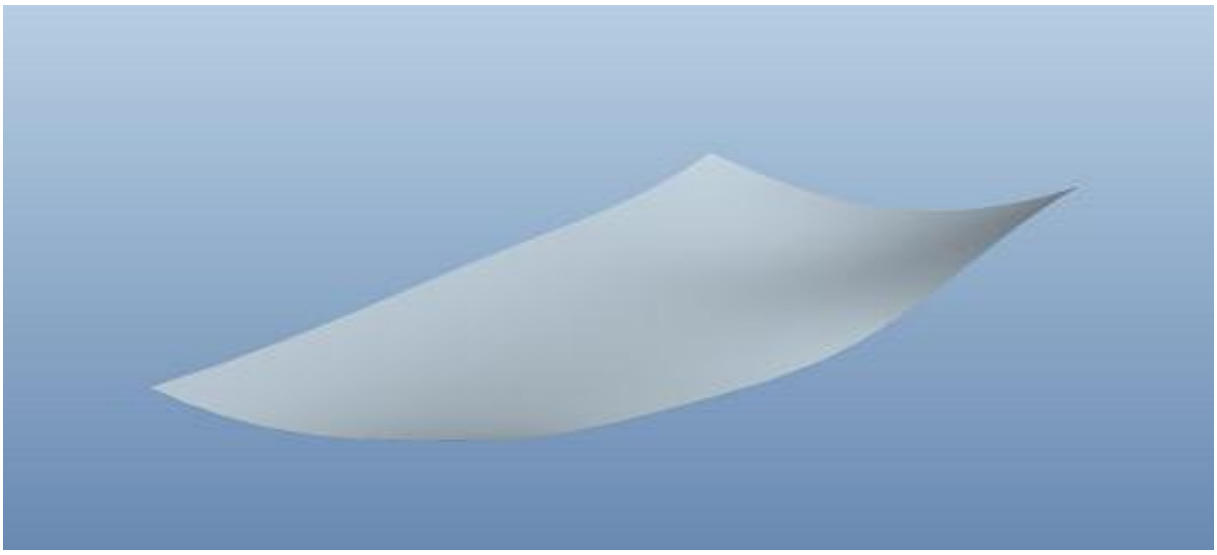

Fig. 5.7 Profile generated in Pro-E

Then the two surfaces are overlapped to compare them. Different views of the overlapped surface are shown in Fig. 5.8(a) and 5.8(b).

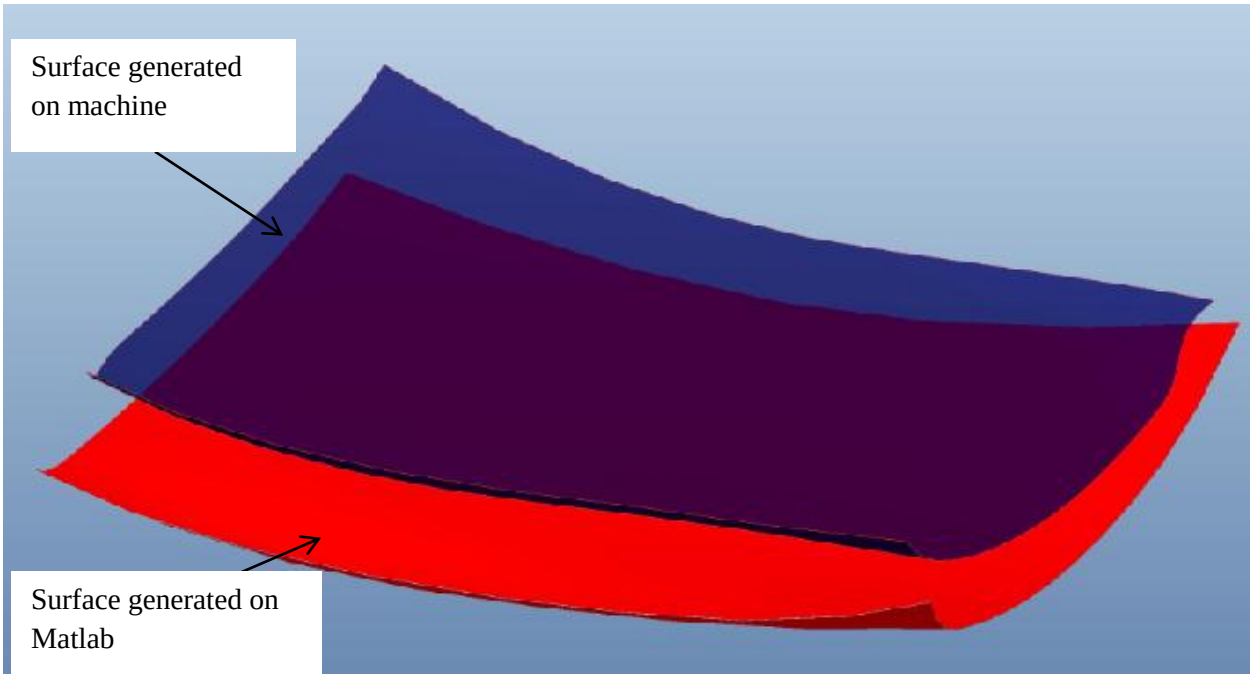

Fig. 5.8(a) Overlapped surfaces: view 1

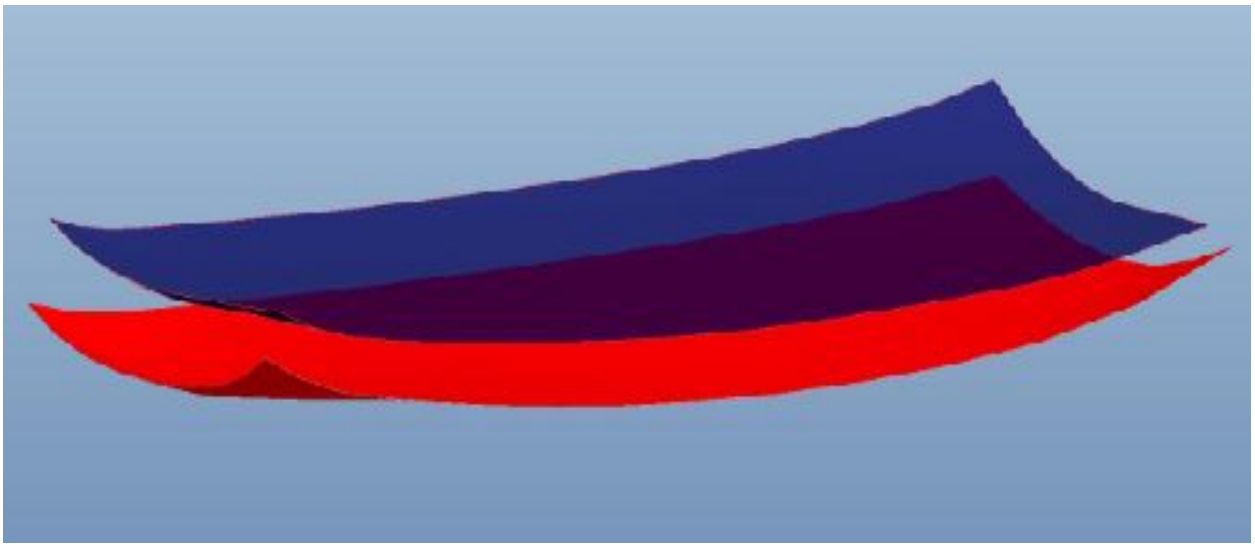

Fig. 5.8(b) Overlapped surfaces: view 2

From the above overlapped figures, it can be seen that the required and generated surfaces are nearly same. But it is important to know the variation between these surfaces. So for measuring the deviation between both the surfaces percentage error is calculated at different points for randomly selected three different tool paths.

The curvature of both the surfaces is compared for toolpath 1 at different break points as shown in Fig. 5.9. The percentage error is calculated for both the curvatures as shown in Table 5.1.

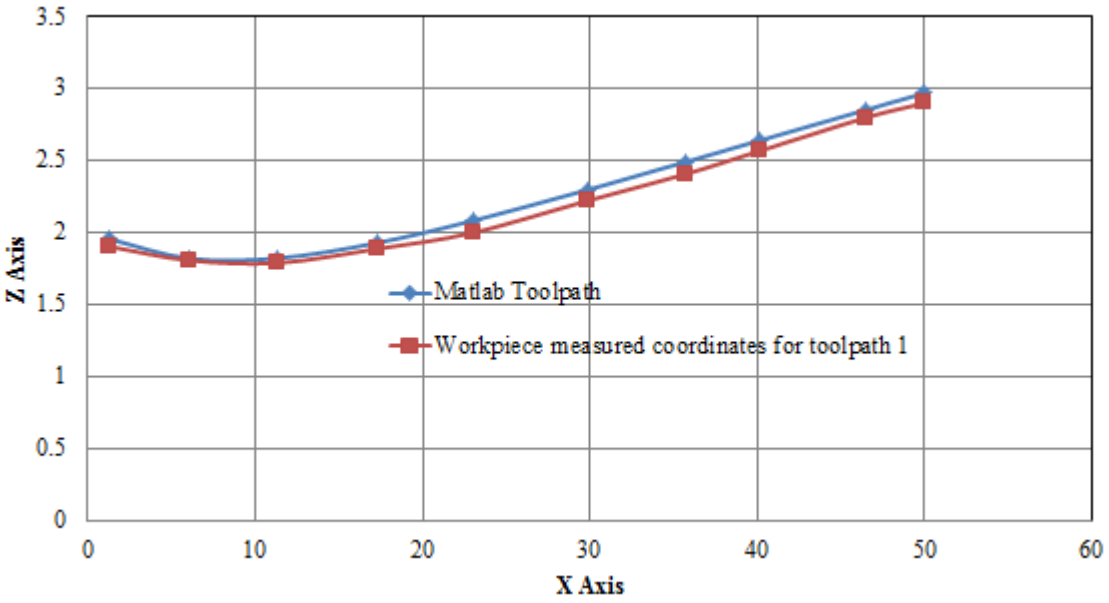

Fig. 5.9 Comparison for tool path 1

Table 5.1 Comparison table to determine the percentage error for toolpath 1

Surface x-coordinate	Matlab surface Z-coordinate	Machined surface Z-coordinate	% error
1.26872	1.95748	1.9054	2.660564
6.07075	1.82238	1.8089	0.739692
11.31575	1.82358	1.7908	1.797563
17.27227	1.93048	1.8887	2.164229
23.01164	2.08518	2.001	4.037062
29.81843	2.29773	2.222	3.295862
35.73592	2.49307	2.40897	3.373351
40.11137	2.63962	2.5678	2.720846
46.5272	2.8545	2.8009	1.877737
50	2.97	2.9008	2.329966

The curvature of both the surfaces is compared for toolpath 10 at different break points as shown in Fig. 5.10. The percentage error is calculated for both the curvatures as shown in Table 5.2.

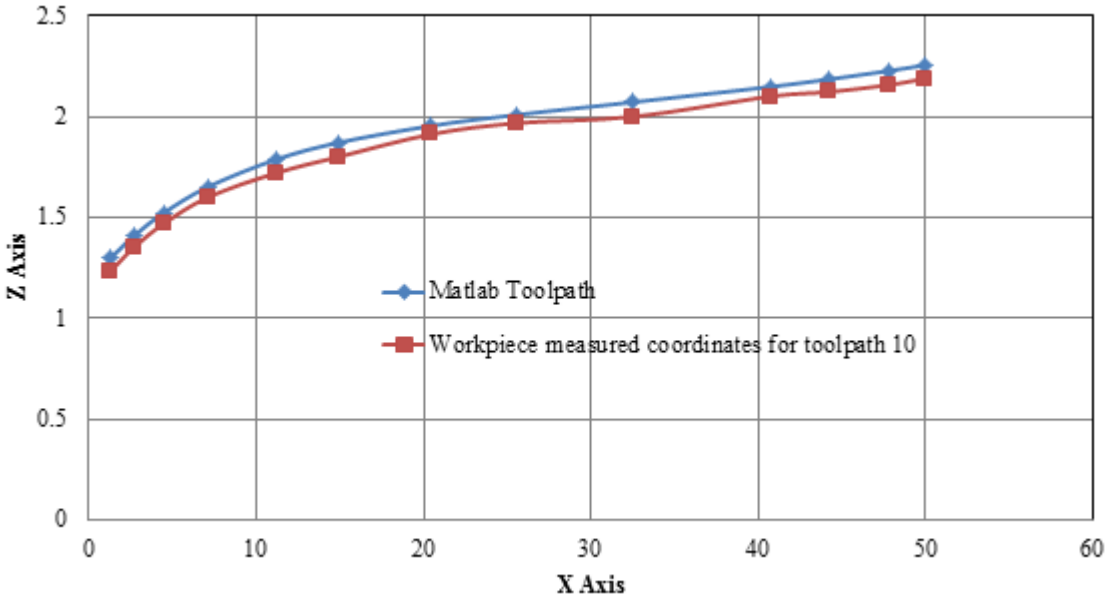

Fig. 5.10 Comparison for tool path 10

Table 5.2 Comparison table to determine the percentage error for toolpath 10

Surface x-coordinate	Matlab surface Z-coordinate	Machined surface Z-coordinate	% error
1.26876	1.2965	1.23	5.129194
2.66936	1.4071	1.35	4.057992
4.47797	1.52283	1.47	3.469199
7.11418	1.65133	1.6	3.108404
11.17727	1.78727	1.72	3.763841
14.89735	1.87058	1.8	3.773161
20.44072	1.95406	1.9123	2.137089
25.59409	2.00922	1.9678	2.061497
32.45135	2.07091	1.999	3.472387
40.75002	2.14837	2.1	2.251474
44.19251	2.18494	2.1223	2.866898
47.77845	2.22692	2.1567	3.153234
50	2.25515	2.189	2.933286

The curvature of both the surfaces is compared for toolpath 25 at different break points as shown in Fig. 5.11. The percentage error is calculated for both the curvatures as shown in Table 5.3.

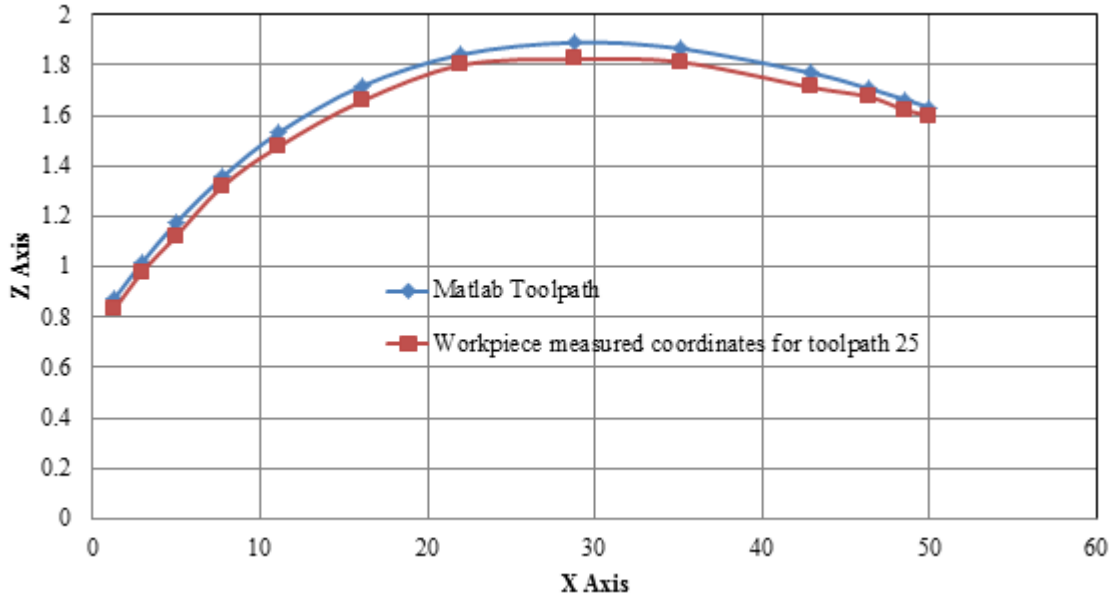

Fig. 5.11 Comparison for tool path 25

Table 5.3 Comparison table to determine the percentage error for toolpath 25

Surface x-coordinate	Matlab surface Z-coordinate	Machined surface Z-coordinate	% error
1.31839	0.87709	0.8345	4.85583
2.938	1.01692	0.978	3.827243
4.94923	1.17209	1.12	4.444198
7.7641	1.35693	1.32	2.721585
11.14321	1.53377	1.478	3.636138
16.0616	1.71624	1.657	3.451732
22.01773	1.84202	1.8	2.281191
28.73775	1.88939	1.8234	3.492662
35.10487	1.86544	1.812	2.86474
42.84849	1.76956	1.7123	3.235833
46.3412	1.70746	1.675	1.901069
48.51614	1.6638	1.6222	2.500301
50	1.632	1.6	1.960784

By comparing both the surfaces (the surface generated by MATLAB and the surface machined on the workpiece) for different toolpaths, it is found that the percentage error between the profile of both the surfaces is less than 5%.

CHAPTER 6
CONCLUSION AND FUTURE SCOPE

6.1 CONCLUSION

In the present study, a novel method, given by Lartigue *et al*. [16], to generate a CNC tool path for a smooth free-form surface in terms of planar cubic B-spline curves is discussed. The only procedure that employs approximation in the entire algorithm is the interpolation of the break points where break points were chosen such that break points reflect the curvature of the surface-plane intersection curve. The pick feed was evaluated so that the maximum scallop height along a scallop curve coincides with the prescribed tolerance. Since the method does not depend on discrete sampling, approximation in determining the pick feed, nor linear approximation of the surface-plane intersection curve, it is more accurate method. The discussed algorithm was used to write a program code in Matlab which was used to machine a component of mild steel. The present work extended the algorithm given by Lartigue *et al*. [16] by actually machining a component on vertical CNC milling machine. It is found that the percentage variation of the actual and machined surface is maximum upto 5% for the different toolpaths generated.

6.2 FUTURE SCOPE

The present work can be extended to free form surface with tangent discontinuity. The present algorithm can be modified using Bezier surface and the results can be compared.

REFERENCES

1. Wang WP, Wang KK, Geometric Modeling for Swept Volume of Moving Solids, Computer Graphics and Applications, vol. 6,8-17, 1986.
2. Loney GC, Ozsoy TM, NC Machining of Free-Form Surfaces, Computer Aided Design, vol. 2, 85-90, 1987.
3. Kuragano T, Sasaki N, Kikuchi A, The Fresdam System for Designing and Manufacturing Free-Form Objects, Flexible Automation, vol. 2, 931-938, 1988.
4. Grewal BS, Numerical Methods in Engineering and Science, Khanna Publication, New Delhi, 1991.
5. Zhou J, Sherbrooke EC, Patrikalakis NM, Computation of Stationary Points of Distance Functions, Engineering with Computers, vol.9, 231-246, 1993.
6. Shpitalni M, Koren Y, Lo CC, Realtime Curve Interpolators, Computer Aided Design, vol. 11, 832-838, 1994.
7. Yang DCH, Kong T, Parametric Interpolator versus Linear Interpolator for Precision CNC Machining, Computer Aided Design, vol. 3, 225-234, 1994.
8. Maekawa T, Patrikalakis NM, Interrogation of Differential Geometry Properties for Design and Manufacture, The Visual Computer, vol. 4,216-237, 1994.
9. Kim KI, Kim K, A New Machine Strategy for Sculptured Surfaces using Offset Surface, International Journal of Production Research, vol. 6, 1683-1697, 1995.
10. Maekawa T, Computation of Shortest Paths on Free-Form Parametric Surfaces, Journal of Mechanical Design, vol. 118,499-508, 1996.
11. Lin RS, Koren Y, Efficient Tool-Path Planning for Machining Free-Form Surfaces, Journal of Engineering for Industry, vol. 118, 20-28, 1996.
12. Sarma R, Dutta D, The Geometry and Generation of NC Tool Paths, Journal of Mechanical Design, vol. 119, 253-258, 1997.
13. Dragomatz D, Mann S, A Classified Bibliography of Literature on NC Milling Path Generation, Computer Aided Design, vol. 29, 239-247, 1997.
14. Hu CY, Maekawa T, Patrikalakis NM, Ye X, Robust Interval Algorithm for Surface Intersections, Computer Aided Design, vol. 29, 617-627, 1997.
15. Ye X, Maekawa T. Differential Geometry of Intersection Curves of Two Surfaces. Computer Aided Geometric Design, vol.16, 767-788, 1999.

16. Lartigue C, Thiebaut F, Maekawa T, CNC Tool Path in Terms of B-spline Curves, Computer Aided Design, vol. 33, 307-319, 2001.
17. Feng HY, Huiwen Li, Constant Scallop Height Tool Path Generation for Three Axis Sculptured Surface Machining, Computer Aided Design, vol. 34, 647-654, 2001.
18. Koren Y, Computer Control of Manufacturing System, Tata McGraw-Hill, New Delhi, 2005.
19. Chen ZC, Song D, A Practical Approach to Generating Accurate Iso-Cusped Tool Paths for Three-Axis CNC Milling of Sculptured Surface Parts, Journal of Manufacturing Processes, vol. 8, 29-37, 2006.
20. Lasemi A, Deyi X, Peihua G, Recent Development in CNC Machining of Freeform Surfaces, Computer Aided Design, vol. 42, 641-654, 2010.